

Supporting Information

Ni(II), Cu(II) and Zn(II) Complexes with 1-Trifluoroethoxyl-2,9,10-trimethoxy-7-oxoaporphine Ligand Simultaneously Target Microtubule and Mitochondria for Cancer Therapy

Lan-Shan Liao, Yin Chen, Zu-Yu Mo, Cheng Hou, Gui-Fa Su*, Hong Liang*, Zhen-Feng Chen*

Contents:

Pages 2–8 The detailed synthetic procedures of ligand (**L**).

Pages 8–13 The experimental methods.

Pages 13–17 Selected bond lengths and angles of **L** and complexes **1–3** with bonded atoms; crystal data and structure refinement details for **L** and complexes **1–3**.

Pages 18–20 ESI-MS spectra of **L** and synthetic intermediate compounds (**1**)–(**7**).

Pages 21 ESI-MS spectra of complexes **1–3**.

Pages 22–27 ¹H-NMR and ¹³C-NMR spectrum of **L** and synthetic intermediate compounds (**1**)–(**7**).

Page 28 ¹H-NMR of complex **3**.

Pages 28–29 UV-Vis absorption spectra of complexes **1–3**.

Page 30 HPLC spectra for complexes **1–3** in DMSO stock solution.

Page 31 HPLC spectra for complexes **1–3** in TBS solution.

Page 32 The DFT calculated HOMO-LUMO gap of complexes **1–3** at

M06-L/def2svp level of theory.

Page 32 The metal amount (Ni, Cu or Zn) of T-24 cancer cells in different organelles was determined by ICP-MS.

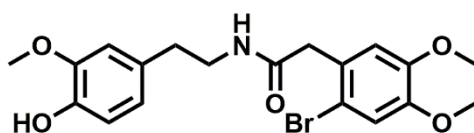
Page 33 Cell cycle analysis by flow cytometry for T-24 cells.

Page 34 *In vivo* anticancer activity of complex **3** in mice bearing T-24 xenograft.

The detailed synthetic procedures of ligand 1-trifluoroethoxyl-2,9,10-trimethoxy-7-oxoaporphine (L):

Synthesis of

2-(2-bromo-4,5-dimethoxyphenyl)-N-[2-(4-hydroxy-3-methoxyphenyl)ethyl]acetamide (1)



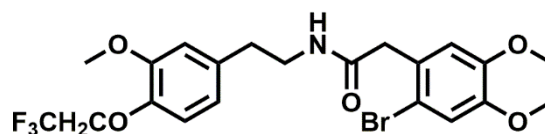
2-Bromo-4,5-dimethoxyphenylacetic acid (6.30 g, 22.9 mmol) and HBTU (9.56 g, 25.2 mmol) were combined in anhydrous dimethylformamide (200 mL), and the reaction stirred at room temperature for 30 min, then 4-hydroxy-3-methoxyphenethylamine hydrochloride (4.70 g, 22.9 mmol) and diisopropylethylamine (11.85 g, 16 mL, 91.7 mmol) were added, and the reaction was stirred at room temperature for 9 h. The reaction was diluted with ethyl acetate, and washed with 2N hydrochloric acid, sodium bicarbonate solution, and brine, then the organic layer was dried over anhydrous Na₂SO₄, the ethyl acetate was removed under

reduced pressure to give compound **1** as white powder (8.4 g, 87%). ESI-MS m/z : 423.4 $[M + H]^+$; 1H NMR (400 MHz, $CDCl_3$) δ 6.97 (s, 1H), 6.75 (t, $J = 4.0$ Hz, 2H), 6.61 (d, $J = 1.8$ Hz, 1H), 6.53 (d, $J = 8.0$ Hz, 1H), 5.63 (s, 1H), 5.48 (t, $J = 5.8$ Hz, 1H), 3.86 (s, 3H), 3.83 (s, 3H), 3.82 (s, 3H), 3.57 (s, 2H), 3.44 (q, $J = 6.8$ Hz, 2H), 2.68 (t, $J = 6.9$ Hz, 2H); ^{13}C NMR (100 MHz, $CDCl_3$) δ 168.90, 147.93, 147.69, 145.61, 143.21, 129.24, 125.47, 120.27, 114.52, 113.71, 113.33, 112.70, 110.03, 55.17, 55.07, 54.86, 42.61, 39.78, 33.97.

Synthesis

of

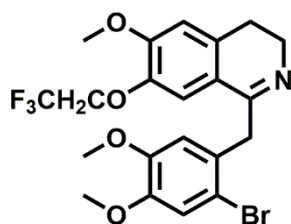
2-(2-bromo-4,5-dimethoxyphenyl)-N-[2-(4-trifluoroethoxy-3-methoxyphenyl)ethyl]acetamide (**2**)



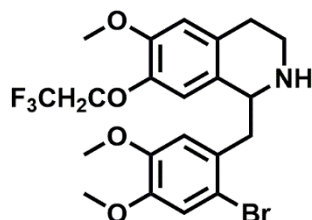
Compound **1** (7.15 g, 16.55 mmol) and cesium carbonate (14 g, 42.97 mmol) were combined in anhydrous DMF (200 mL), and stirred at 60 °C for 30 min. The 1,1,1-trifluoro-2-iodoethane (7 g, 33.34 mmol) was added slowly, and the reaction was stirred at room temperature for 8 h. The reaction was diluted with ethyl acetate, washed with a sodium bicarbonate solution and brine, dried over anhydrous Na_2SO_4 , and the solvent was removed under reduced pressure to give compound **2** as white powder (6.9 g, 82%). ESI-MS m/z : 505.5 $[M + H]^+$; 1H NMR (400 MHz, $CDCl_3$) δ 6.97 (s, 1H), 6.82 (d, $J = 8.1$ Hz, 1H), 6.77 (d, $J = 7.4$ Hz, 1H), 6.66 (s, 1H), 6.56 (d, $J = 8.1$ Hz, 1H), 5.44 (s, 1H), 4.35 (q, $J = 8.4$ Hz, 2H), 3.87 (s, 3H), 3.83 (s, 3H), 3.82 (s, 3H), 3.58 (s, 2H), 3.48 – 3.44 (m, 2H), 2.74 (d, $J = 4.3$ Hz, 2H); ^{13}C NMR (100

MHz, CDCl₃) δ 168.81, 149.42, 147.95, 147.70, 144.60, 133.56, 125.46, 119.76, 116.67, 114.50, 113.69, 112.69, 111.89, 67.20, 66.85, 55.11, 55.07, 54.88, 42.63, 39.54, 34.02.

Synthesis **of**
1-(2-bromo-4,5-dimethoxybenzyl)-7-trifluoroethoxyl-6-methoxy-3,4-dihydroisoquinoline (3)

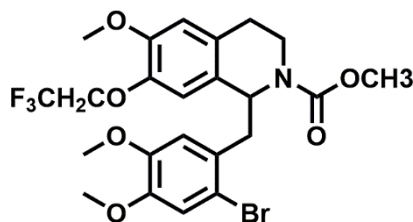


Compound **2** (9.19 g, 18.2 mmol) was dissolved in acetonitrile (100 mL), and phosphorus oxychloride (13.98 g, 8.4 mL, 91.2 mmol) was added slowly. The reaction was stirred at 90 °C for 4 h. After 4 h of complete reaction, the reaction was slowly cooled to room temperature, and the ice water was slowly added for quenching, then ammonia water is added until pH was 8 to 9. The solution was extracted with dichloromethane, and dried over Na₂SO₄, the dichloromethane was removed under reduced pressure. Compound **3** was recrystallized from methanol (6.38 g, 72%). ESI-MS *m/z*: 487.5 [M + H]⁺; ¹H NMR (400 MHz, DMSO-*d*₆) δ 7.29 (s, 1H), 7.09 (s, 1H), 6.97 (s, 1H), 6.87 (s, 1H), 4.68 (t, *J* = 9.0 Hz, 2H), 4.04 (s, 2H), 3.83 (s, 3H), 3.74 (s, 3H), 3.67 (s, 3H), 3.50 – 3.46 (m, 2H), 2.60 – 2.56 (m, 2H); ¹³C NMR (100 MHz, CDCl₃) δ 194.79, 163.81, 152.81, 152.50, 148.58, 145.35, 134.52, 131.52, 124.76, 121.99, 119.46, 115.99, 115.79, 113.70, 111.37, 68.05, 67.70, 56.40, 56.16, 48.09, 25.17.

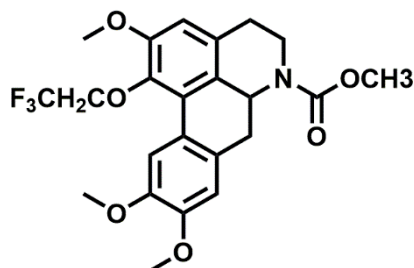
1-(2-bromo-4,5-dimethoxybenzyl)-7-trifluoroethoxyl-6-methoxy-1,2,3,4-tetrahydroisoquinoline (4)

Compound **3** (11.5 g, 23.61 mmol) was dissolved in methanol (100 mL), and sodium borohydride (1.81 g, 48.2 mmol) was added slowly, then the reaction was stirred at room temperature for 9 h. The methanol was removed under reduced pressure, and the aqueous solution was extracted with dichloromethane. The reaction was dried over Na_2SO_4 , the dichloromethane was removed under reduced pressure to obtain compound **4** (7.5 g, 65%). ESI-MS m/z : 489.5 $[\text{M} + \text{H}]^+$; ^1H NMR (400 MHz, $\text{DMSO-}d_6$) δ 7.11 (s, 1H), 6.90 (s, 1H), 6.78 (d, $J = 23.1$ Hz, 2H), 5.35 – 5.18 (m, 1H), 4.61 (dd, $J = 19.2, 9.4$ Hz, 2H), 3.77 (s, 3H), 3.75 (s, 3H), 3.66 (d, $J = 15.9$ Hz, 3H), 3.51 (s, 1H), 3.20 (s, 2H), 3.16 – 2.95 (m, 2H), 2.78 – 2.58 (m, 2H); ^{13}C NMR (100 MHz, $\text{DMSO-}d_6$) δ 155.66, 155.38, 148.63, 148.26, 145.11, 129.76, 129.22, 128.51, 115.62, 114.98, 114.76, 114.45, 113.13, 56.16, 54.18, 52.81, 52.36, 41.48, 38.36, 37.53, 27.93.

Synthesis of 6-carbomethoxy-1-trifluoroethoxyl-2, 9, 10-trimethoxynoraporphine (6)



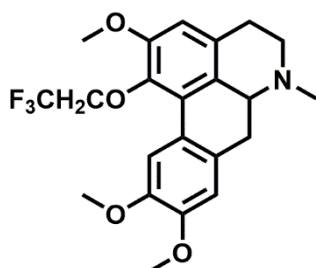
The compound **4** (11.6 g, 23.7 mmol) was dissolved in chloroform (25 mL), sodium hydroxide aqueous solution (25 mL, 2 mol/L) was added under ice bath, methyl chloroformate (3.36 g, 35.6 mmol) was added dropwise, and the reaction stirred at room temperature for 5 h. The organic layer was washed by sodium bicarbonate solution three times, the combined organic extracts was dried over Na₂SO₄, and the solvent was removed under reduced pressure to obtain crude product **5** and proceeded to the next step without further purification.



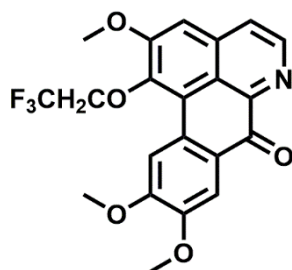
Compound **5** (7 g, 12.80 mmol), phosphorus tricyclohexyl (0.8 g, 2.86mmol), cesium carbonate (15 g, 46.04 mmol), palladium acetate (0.32 g, 1.43 mmol) were combined in DMF (100 mL), the mixture was heated at 165 °C for 8 h under nitrogen. The mixture was filtered under reduced pressure, and the filtrate was extracted with ethyl acetate three times, then the organic layer was dried over Na₂SO₄, the solvent was removed to obtain compound **6** (4.5 g, 41%). ESI-MS *m/z*: 467.7 [M + H]⁺, 489.6 [M + Na]⁺, 505.5 [M + K]⁺; ¹H NMR (400 MHz, Chloroform-*d*) δ 7.96 (s, 1H), 6.79 (s, 1H), 6.65 (s, 1H), 4.72 – 4.67 (m, 1H), 4.47 – 4.34 (m, 2H), 3.93 (s, 3H), 3.90 (s, 6H), 3.77 (s, 3H), 3.01 – 2.62 (m, 6H). ¹³C NMR (100 MHz, CDCl₃) δ 150.04, 147.54,

146.44, 141.04, 129.99, 128.71, 127.03, 124.81, 123.69, 122.30, 120.92, 111.09, 110.11, 109.92, 68.08, 67.74, 55.06, 54.78, 54.56, 51.70, 50.89, 37.98, 29.30.

Synthesis of 1-trifluoroethoxyl-2,9,10-trimethoxy-7-oxoaporphine (L)



Compound **6** (6.2 g, 13.27 mmol) was dissolved in tetrahydrofuran (80 mL), and LiAlH_4 (5.58 g, 147.04 mmol) was slowly added under ice bath, then the mixture was stirred at rt for 0.5 h. After that, the reaction heated at 65 °C for 6 h under nitrogen. After cooling, ammonia water was slowly added with stirring until no bubbles were formed. Filtration under reduced pressure, the filtrate was removed under reduced pressure to give crude product **7** and proceeded to the next step without further purification.



The crude product **7** dissolved in acetic acid (100 mL), $\text{Mn}(\text{OAc})_3 \cdot x\text{H}_2\text{O}$ (46.4 g) was added, stirred at 80 °C for 9 h. The reaction mixture was filtered and the acetic acid was removed under reduced pressure, then the mixture was extracted with dichloromethane three times. The organic layer was dried over Na_2SO_4 , and the solvent was removed under reduced pressure. The obtained crude mixture was

purified by column chromatography on silica gel, using dichloromethane and methanol as eluent to give target ligand **L** as a yellow powder (1.5 g, 27%). ESI-MS m/z : 420 $[M + H]^+$; 1H NMR (400 MHz, DMSO- d_6) δ 8.83 (d, $J = 5.2$ Hz, 1H), 8.48 (s, 1H), 8.04 (d, $J = 5.3$ Hz, 1H), 7.75 (s, 1H), 7.66 (s, 1H), 4.87 (q, $J = 9.1$ Hz, 2H), 4.07 (s, 3H), 3.95 (s, 3H), 3.94 (s, 3H); ^{13}C NMR (100 MHz, DMSO- d_6) δ 180.41, 155.44, 153.71, 149.84, 148.20, 145.13, 145.09, 135.53, 128.32, 126.63, 124.19, 121.00, 119.32, 111.21, 109.48, 107.96, 69.19, 68.85, 57.05, 55.98, 55.75; Elemental analysis calcd (%) for $C_{21}H_{16}F_3NO_5$: C 60.15, H 3.85, N 3.34; Found: C 60.11, H 3.82, N 3.36.

The experimental methods

X-ray crystallographic analysis

The X-ray diffraction analyses for ligand and complexes **1–3** were performed on an Agilent SuperNova CCD diffractometer equipped with graphite monochromated Mo- K_{α} radiation ($\lambda = 0.71073$ Å). Using direct methods, the structures of ligand and metal complexes were solved, and their crystal structure were refined by the full-matrix least-squares method on F^2 with anisotropic thermal parameters using SHELX-97 program.¹ Non-hydrogen atoms were located using Differential Fourier Transforms. Finally, the hydrogen atoms were added theoretically.

Computational details (DFT calculation)

The calculations were performed on Gaussian 16 program Rev. A.03.² Geometry optimizations were carried out with M06-L³ /def2-SVP⁴ level of theory. Frequency

analysis calculations were performed to characterize the structures at the minima (no imaginary frequency). The 3D optimized structure figures in this paper were displayed by IBOview visualization program.⁵

Cellular uptake

T-24 cells were exposed to 10 μ M of complexes **1–3**. After 10 h treatment, trypsin was used to digest and harvest T-24 cells, and PBS was used to rinse T-24 cells. The cell fractions were isolated using the Fraction PERP kit, and the fraction was diluted to the concentration of 5% HNO₃. Finally, the metal content in T-24 cells was detected by ICP-MS.

Mitochondrial membrane potential detection

After T-24 cells were exposed to complexes **1–3** at different concentrations, the cells were collected with PBS, and incubated with 500 μ L JC-1 working solution for 0.5 h at 37 °C. After discarding the staining solution, the T-24 cells were washed by JC-1 staining buffer. Ultimately, the $\Delta\psi$ was detected by flow cytometry.

Detection of cellular ATP levels

When the tumor cells were treated with complexes **1–3** for 24 h, the cells were sufficiently lysed and centrifuged at 12,000 \times g for 5 minutes in a centrifuge. 100 μ L of ATP detection working diluent was added to the 96-well, and 20 μ L of cell supernatant also was added to the 96-well, followed by quick mixing. Luminance was measured by cell imaging multi-mode reader.

Mitochondrial staining

When T-24 cells grew to 70% confluence in a petri dish, the cells were treated with drug for 24 h. Subsequently, the cells were washed twice with sterile PBS, and then incubated with 0.2 μ M Mito-Tracker Green for 0.5 h at 37 °C. The fluorescent images were obtained by fluorescence microscopy.

Measurement of ROS generation

DCFH-DA is a fluorescent probe, which is used to detect the level of ROS. DCFH-DA can pass through cell membranes and be deacetylated by intracellular esterase. As a result, the fluorescent DCFH-DA is converted to the non-fluorescent DCFH that cannot pass through the cell membrane and is oxidized into the fluorescent DCF by the intracellular ROS. T-24 cells were firstly exposed to complexes 1–3, followed by trypsin digestion to harvest T-24 cells and PBS rinse. The T-24 cells were incubated with DCFH-DA for 0.5 h at 37 °C. After the DCFH-DA was discarded, serum-free cell culture medium was used to wash T-24 cells three times. Finally, the T-24 cells were detected by flow cytometry.

Intracellular Ca²⁺ measurement

Fluo-3 AM is a fluorescent probe for detecting the concentration of intracellular free Ca²⁺. Fluo-3 AM has a weak fluorescence, but it can penetrate the cell membrane and be cleaved by esterase into Fluo-3. The combination of Fluo-3 and intracellular Ca²⁺ in cell can produce strong fluorescence. Therefore, the levels of Ca²⁺ in the cell were determined by the fluorescence intensity of Fluo-3. After treatment with complexes 1–3, trypsin was used to digest and harvest T-24 cells, and PBS was used to rinse T-24 cells. The cells were incubated with Fluo-3 AM (5.0 mM) and placed in an incubator

for 0.5 h at 37 °C under dark environment. Finally, the intracellular free Ca²⁺ was detected by a flow cytometer.

Measurement of caspase-3/9 activity

Using the CaspGLOW™ staining kit, the caspase-9/3 activities were determined. After treatment with complexes 1–3, the cells were collected and washed thrice with PBS, followed by incubation with 1 μL FITC-LEHD-FMK (for caspase-9) or 1 μL of FITC-DEVD-FMK (for caspase-3) for 0.5 h. Ultimately, the T-24 cells were detected by a flow cytometer.

Immunofluorescence assay

After exposure of complexes 1–3 for 24 h, 4% paraformaldehyde was used to fix the T-24 cells for 60 min, and 0.1% triton X-100 was used to permeabilize the cells for 30 min. T-24 cells incubated with the immunostaining blocking solution for 60 min, then incubated with anti-β-tubulin. Subsequently, the cells were incubated with fluorescence-labeled secondary antibody for 60 min. Nuclei were stained with Hoechst 33324. Finally, the T-24 cells were imaged by fluorescence microscopy.

Western blotting

The T-24 cells were incubated with complexes 1–3 at three different concentrations, and the total cellular proteins of the tumor cells were acquired by lysing in the lysis buffer. Total protein extracts were added into each lane of 10% SDS-PAGE gels, separated by electrophoresis and transferred to a PVDF membrane. Hereafter, the PVDF membranes were blocked with skim milk for 1 h and incubated with primary antibodies in the refrigerator for 9 h. The PVDF membranes further incubated with

secondary antibodies at rt for 1–2 h. Finally, the immunoreactive signal of PVDF membranes were detected.

Cell apoptosis

The T-24 cells were treated with complexes **1–3**. After 24 h treatment, the T-24 cells were re-suspended in 500 μ L binding buffer. Hereafter, the suspended cells were subjected to 5 μ L PI and 5 μ L FITC Annexin V for 0.5 h. Finally, the T-24 cells immediately were examined by flow cytometry.

References

- [1] G. M. Sheldrick, SHELXS-97, Program for the solution of crystal structures, University of Göttingen, Göttingen, Germany, 1997.
- [2] M. J. Frisch, G. W. Trucks, H. B. Schlegel, G. E. Scuseria, M. A. Robb, J. R. Cheeseman, G. Scalmani, V. Barone, G. A. Petersson, H. Nakatsuji, X. Li, M. Caricato, A. V. Marenich, J. Bloino, B. G. Janesko, R. Gomperts, B. Mennucci, H. P. Hratchian, J. V. Ortiz, A. F. Izmaylov, J. L. Sonnenberg, F. Ding, F. Lipparini, F. Egidi, J. Goings, B. Peng, A. Petrone, T. Henderson, D. Ranasinghe, V. G. Zakrzewski, J. Gao, N. Rega, G. Zheng, W. Liang, M. Hada, M. Ehara, K. Toyota, R. Fukuda, J. Hasegawa, M. Ishida, T. Nakajima, Y. Honda, O. Kitao, H. Nakai, T. Vreven, K. Throssell, J. A. Montgomery Jr., J. E. Peralta, F. Ogliaro, M. J. Bearpark, J. J. Heyd, E. N. Brothers, K. N. Kudin, V. N. Staroverov, T. A. Keith, R. Kobayashi, J. Normand, K. Raghavachari, A. P. Rendell, J. C. Burant, S. S. Iyengar, J. Tomasi, M. Cossi, J. M. Millam, M. Klene, C. Adamo, R. Cammi, J. W. Ochterski, R. L. Martin, K. Morokuma, O. Farkas, J.

B. Foresman, D. J. Fox, Gaussian 16 Rev. A.03. 2016.

[3] Y. Zhao, D. G. Truhlar, Density functionals with broad applicability in chemistry,

Accounts Chem. Res., 2008, **41**, 157–167.

[4] F. Weigend, R. Ahlrichs, Balanced basis sets of split valence, triple zeta valence and quadruple zeta valence quality for H to Rn: Design and assessment of accuracy, *Phys. Chem. Chem. Phys.*, 2005, **7**, 3297–3305.

[5] G. Knizia, J. E. M. N. Klein, Electron flow in reaction mechanisms-revealed from first principles, *Angew. Chem. Int. Ed.*, 2015, **54**, 5518–5522.

Table S1. Selected bond lengths and angles of ligand with bonded atoms

F1–C21	1.328 (4)	O5–C20	1.434 (3)
F2–C21	1.333 (4)	N1–C6	1.355 (4)
F3–C21	1.342 (4)	N1–C7	1.343 (3)
O1–C1	1.450 (3)	C2–O1–C1	116.8 (2)
O1–C2	1.370 (3)	C13–O3–C12	116.0 (2)
O2–C9	1.238 (3)	C14–O4–C15	118.21 (19)
O3–C12	1.436 (3)	C19–O5–C20	115.41 (19)
O3–C13	1.383 (3)	C7–N1–C6	117.1 (2)
O4–C14	1.376 (3)	F1–C21–F2	106.4 (3)
O4–C15	1.431 (3)	F1–C21–F3	104.8 (4)
O5–C19	1.394 (3)	F2–C21–F3	107.6 (3)

Table S2. Selected bond lengths and angles of complex 1 with bonded atoms

Ni1–O1	2.063 (3)	O6–Ni1–O6a	180.00 (16)
Ni1–O1a	2.063 (3)	N1–Ni1–O1a	99.78 (13)
Ni1–O6a	2.103 (4)	N1a–Ni1–O1	99.78 (13)
Ni1–O6	2.103 (4)	N1–Ni1–O1	80.22 (13)
Ni1–N1a	2.034 (4)	N1i–Ni1–O1a	80.22 (13)
Ni1–N1	2.034 (4)	N1–Ni1–O6a	93.53 (16)
O1a–Ni1–O1	180.0	N1a–Ni1–O6	93.53 (16)

O1a—Ni1—O6	92.89 (14)	N1—Ni1—O6	86.47 (16)
O1—Ni1—O6	87.11 (14)	N1a—Ni1—O6a	86.47 (16)
O1a—Ni1—O6a	87.11 (14)	N1a—Ni1—N1	180.0
O1—Ni1—O6a	92.89 (14)		

Symmetry code: (a) 1-x, 1-y, 1-z

Table S3. Selected bond lengths and angles of complex 2 with bonded atoms

Cu1—O7	2.392 (5)	O1—Cu1—O1a	180.0
Cu1—O7a	2.392 (5)	N1a—Cu1—O7a	88.0 (2)
Cu1—O1	2.020 (4)	N1a—Cu1—O7	92.0 (2)
Cu1—O1a	2.020 (4)	N1—Cu1—O7	88.0 (2)
Cu1—N1a	1.958 (6)	N1—Cu1—O7a	92.0 (2)
Cu1—N1	1.958 (6)	N1a—Cu1—O1a	82.4 (2)
O7a—Cu1—O7	180.0	N1a—Cu1—O1	97.6 (2)
O1—Cu1—O7a	91.17 (18)	N1—Cu1—O1	82.4 (2)
O1a—Cu1—O7a	88.83 (18)	N1—Cu1—O1a	97.6 (2)
O1a—Cu1—O7	91.17 (18)	N1a—Cu1—N1	180.0 (3)
O1—Cu1—O7	88.83 (18)		

Symmetry code: (a) -x, 2-y, -z

Table S4. Selected bond lengths and angles of complex 3 with bonded atoms

Zn1—O1	2.127 (2)	O6a—Zn1—O6	180.0
Zn1—O1a	2.127 (2)	N1—Zn1—O1	79.13 (9)
Zn1—O6	2.211 (3)	N1—Zn1—O1a	100.87 (9)
Zn1—O6a	2.211 (3)	N1a—Zn1—O1a	79.13 (9)
Zn1—N1a	2.032 (3)	N1a—Zn1—O1	100.87 (9)
Zn1—N1	2.032 (3)	N1a—Zn1—O6	86.76 (11)
O1i—Zn1—O1	180.0	N1a—Zn1—O6a	93.24 (11)
O1—Zn1—O6a	87.71 (9)	N1—Zn1—O6a	86.76 (11)
O1—Zn1—O6	92.29 (9)	N1—Zn1—O6	93.24 (11)
O1a—Zn1—O6a	92.29 (9)	N1—Zn1—N1a	180.0
O1a—Zn1—O6	87.71 (9)		

Symmetry code: (a) 1-x, 1-y, 1-z

Table S5. Crystal data and structure refinement details for ligand (L)

Ligand	L
Empirical formula	C ₂₁ H ₁₆ F ₃ NO ₅
Formula weight	419.35
Temperature/K	296
Crystal system	tetragonal
Space group	<i>I</i> 4 ₁ /a
a/Å	23.545(13)
b/Å	23.545(13)
c/Å	13.805(7)
α/°	90
β/°	90
γ/°	90
Volume(Å ³)	7653(9)
Z	16
D _c (g.cm ⁻³)	1.456
μ (mm ⁻¹)	0.12
F(000)	3456
2θ range for data collection (°)	3.42 to 52.308
Reflections collected	29705
Independent reflections	3820[R(int) = 0.043]
Data/restraint/parameters	3820/0/274
Goodness-of-fit on F ²	1.03
R [I > 2σ(I)]	R1=0.0517,wR2=0.1345
R (all data)	R1=0.0894,wR2=0.1687

Table S6. Crystal data and structure refinement details for complex 1

Compound	Complex 1
Empirical formula	C ₄₂ H ₃₂ F ₆ N ₄ NiO ₁₆
Formula weight	1021.41
Temperature/K	293
Crystal system	triclinic
Space group	P-1
a/Å	7.6971(4)
b/Å	11.4942(9)
c/Å	12.0058(10)
α/°	71.997(7)

$\beta/^\circ$	87.716(6)
$\gamma/^\circ$	77.460(6)
Volume(\AA^3)	985.65(13)
Z	1
D_c ($\text{g}\cdot\text{cm}^{-3}$)	1.721
μ (mm^{-1})	0.61
F(000)	522
2 θ range for data collection ($^\circ$)	6.58 to 52.74
Reflections collected	12325
Independent reflections	4019[R(int) = 0.045]
Data/restraint/parameters	4019/108/316
Goodness-of-fit on F2	1.04
R [$I > 2\sigma(I)$]	R1=0.0727,wR2=0.2049
R (all data)	R1=0.0995,wR2=0.2297

Table S7. Crystal data and structure refinement details for complex 2

Compound	Complex 2
Empirical formula	$\text{C}_{42}\text{H}_{32}\text{CuF}_6\text{N}_4\text{O}_{16}$
Formula weight	1026.27
Temperature/K	293
Crystal system	triclinic
Space group	P-1
a/ \AA	7.8601(8)
b/ \AA	11.264 (3)
c/ \AA	11.987 (3)
$\alpha/^\circ$	73.43 (2)
$\beta/^\circ$	85.658 (16)
$\gamma/^\circ$	76.835 (15)
Volume(\AA^3)	990.4 (4)
Z	1
D_c ($\text{g}\cdot\text{cm}^{-3}$)	1.721
μ (mm^{-1})	0.67
F(000)	523
2 θ range for data collection ($^\circ$)	7.08 to 50.69
Reflections collected	11484
Independent reflections	3637[R(int) = 0.115]
Data/restraint/parameters	3637/0/316

Goodness-of-fit on F2	1.025
R [I > 2σ(I)]	R1=0.0801,wR2=0.1620
R (all data)	R1=0.1823,wR2=0.2273

Table S8. Crystal data and structure refinement details for complex 3

Compound	Complex 3
Empirical formula	C ₄₂ F ₆ N ₄ O ₁₆ ZnH ₃₂
Formula weight	1028.11
Temperature/K	293
Crystal system	triclinic
Space group	P-1
a/Å	7.7839(4)
b/Å	11.4188(6)
c/Å	11.9926(6)
α/°	73.088(5)
β/°	86.180(4)
γ/°	77.830(5)
Volume(Å ³)	996.90(9)
Z	1
D _c (g.cm ⁻³)	1.713
μ (mm ⁻¹)	0.73
F(000)	524
2θ range for data collection (°)	7.04 to 52.74
Reflections collected	12086
Independent reflections	4072[R(int) = 0.051]
Data/restraint/parameters	4072/0/316
Goodness-of-fit on F2	1.06
R [I > 2σ(I)]	R1=0.0569,wR2=0.1295
R (all data)	R1=0.0860,wR2=0.1505

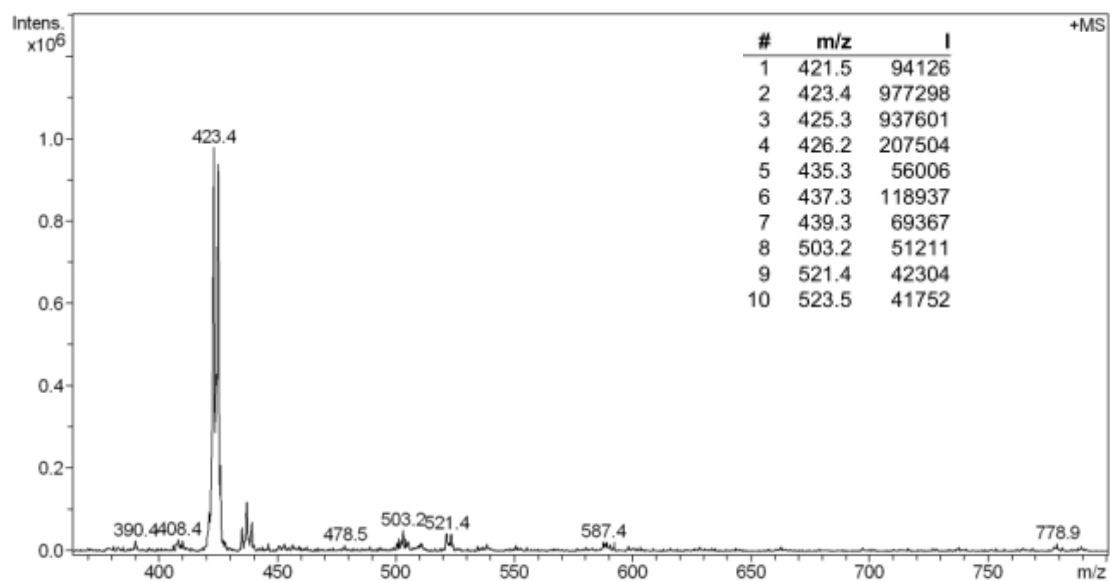


Figure S1. MS-EI spectra of (1)

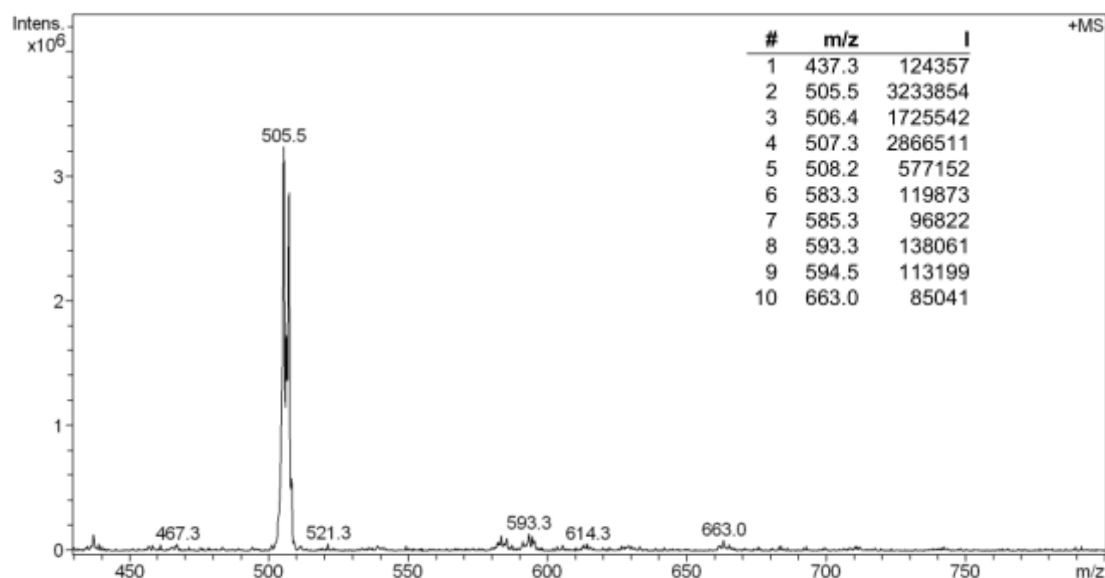


Figure S2. MS-EI spectra of (2)

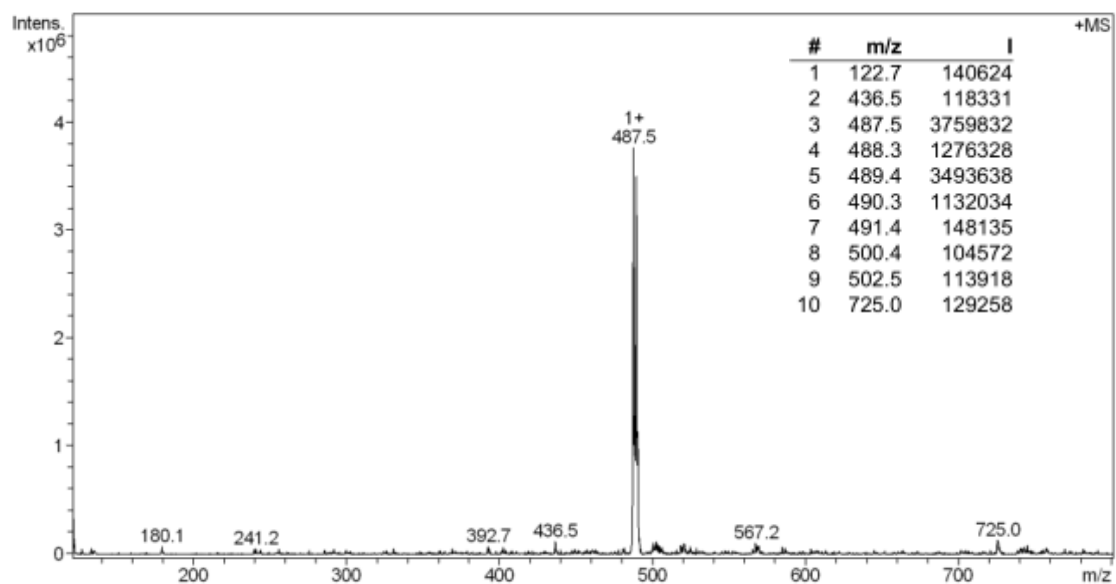


Figure S3. MS-EI spectra of (3)

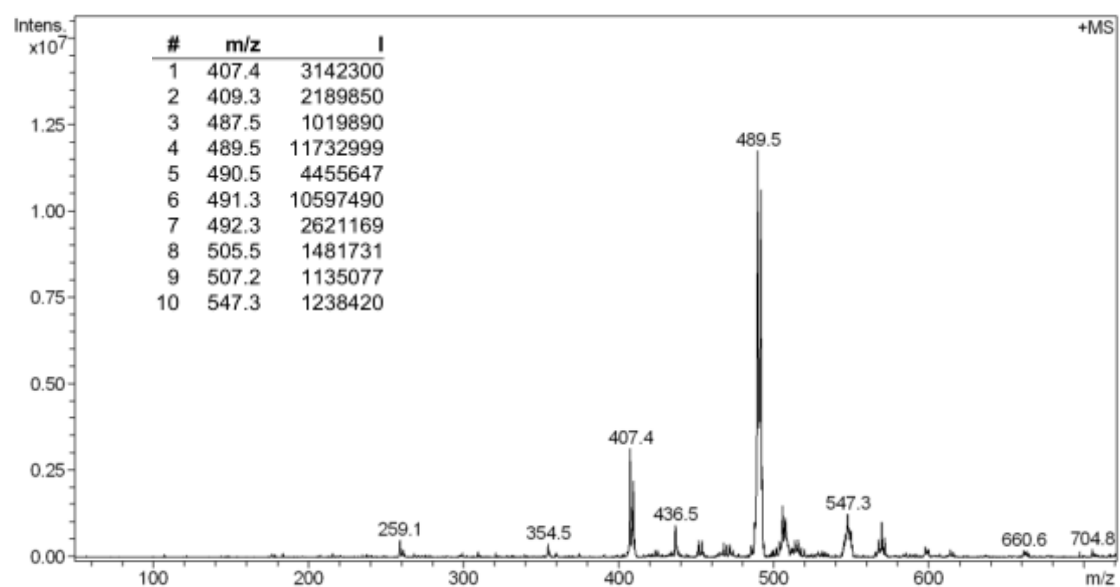


Figure S4. MS-EI spectra of (4)

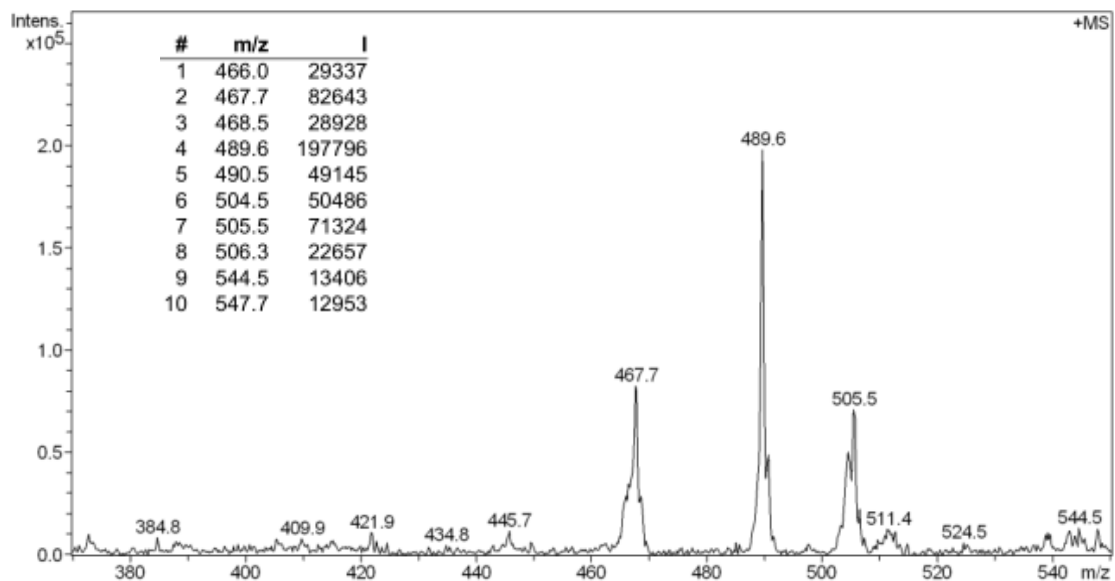


Figure S5. MS-EI spectra of (6)

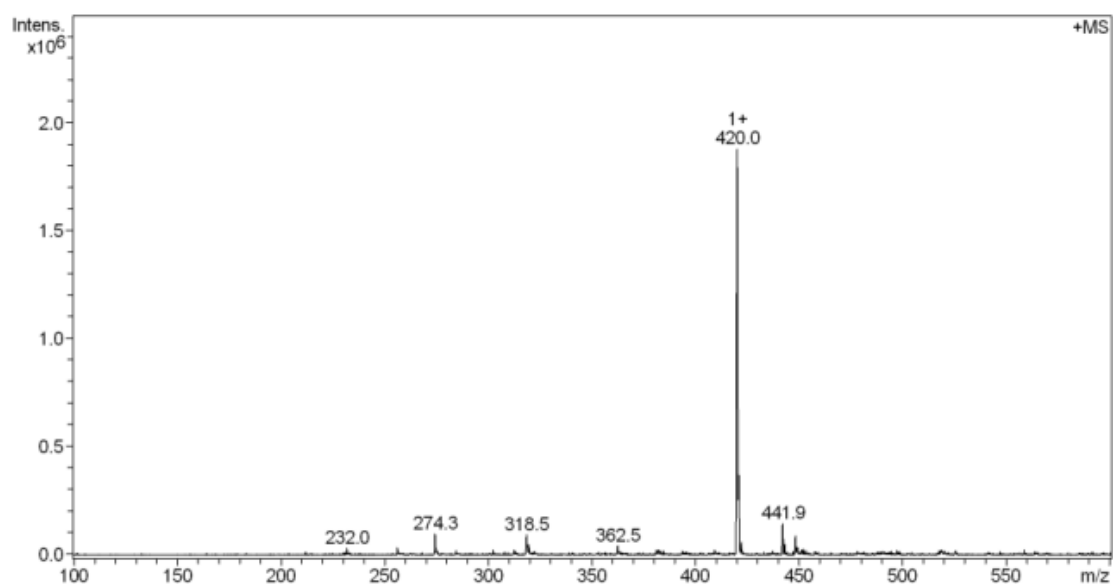


Figure S6. MS-EI spectra of L

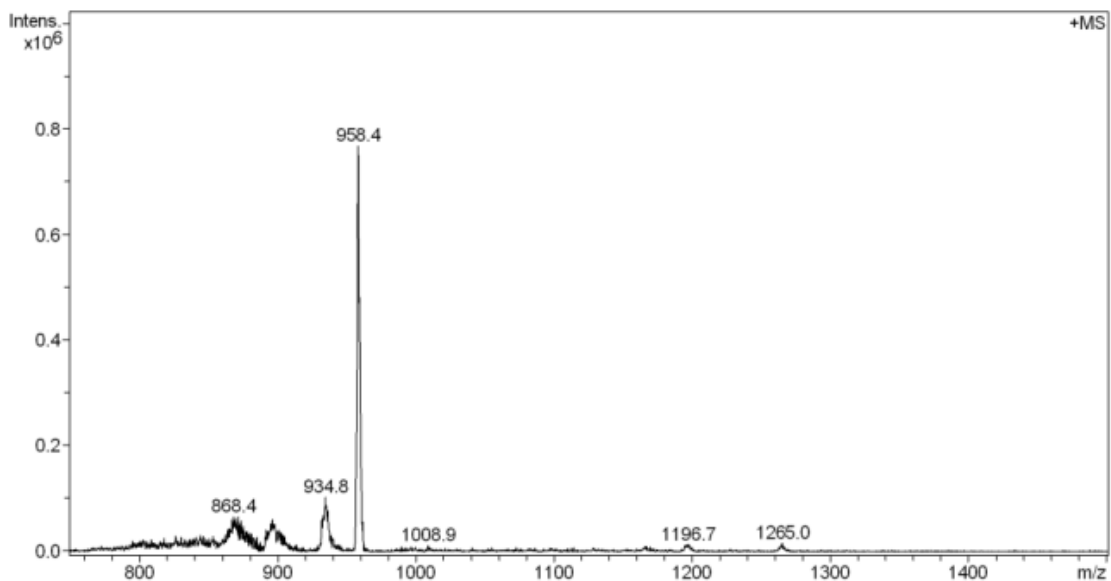


Figure S7. MS-EI spectra of complex 1

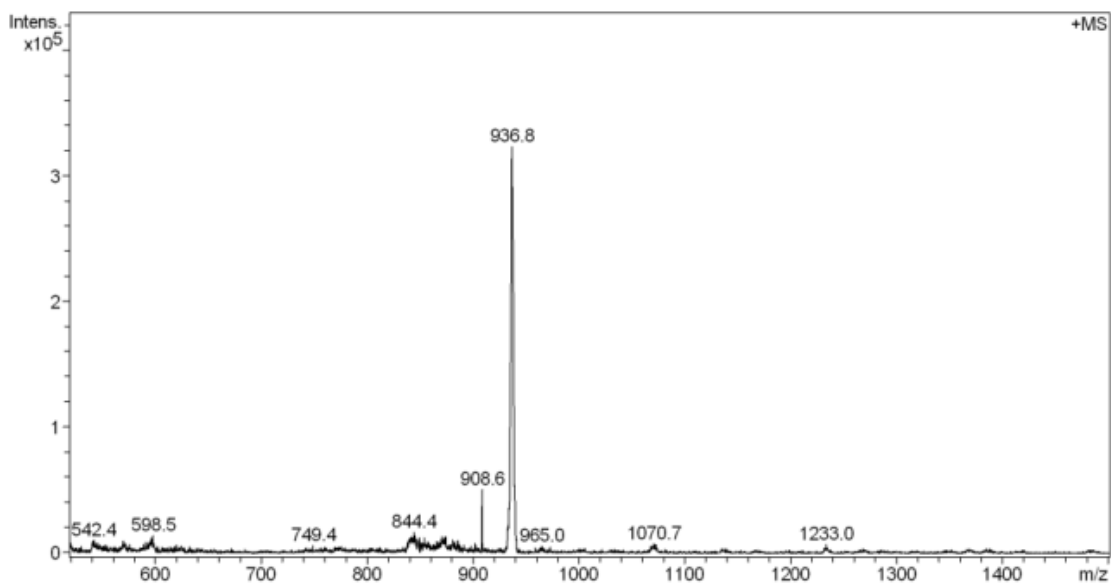


Figure S8. MS-EI spectra of complex 2

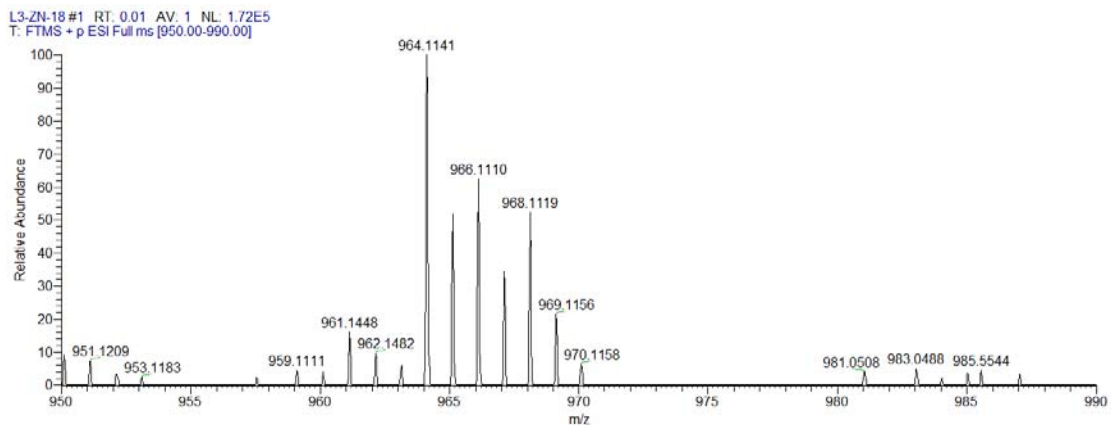


Figure S9. MS-EI spectra of complex 3

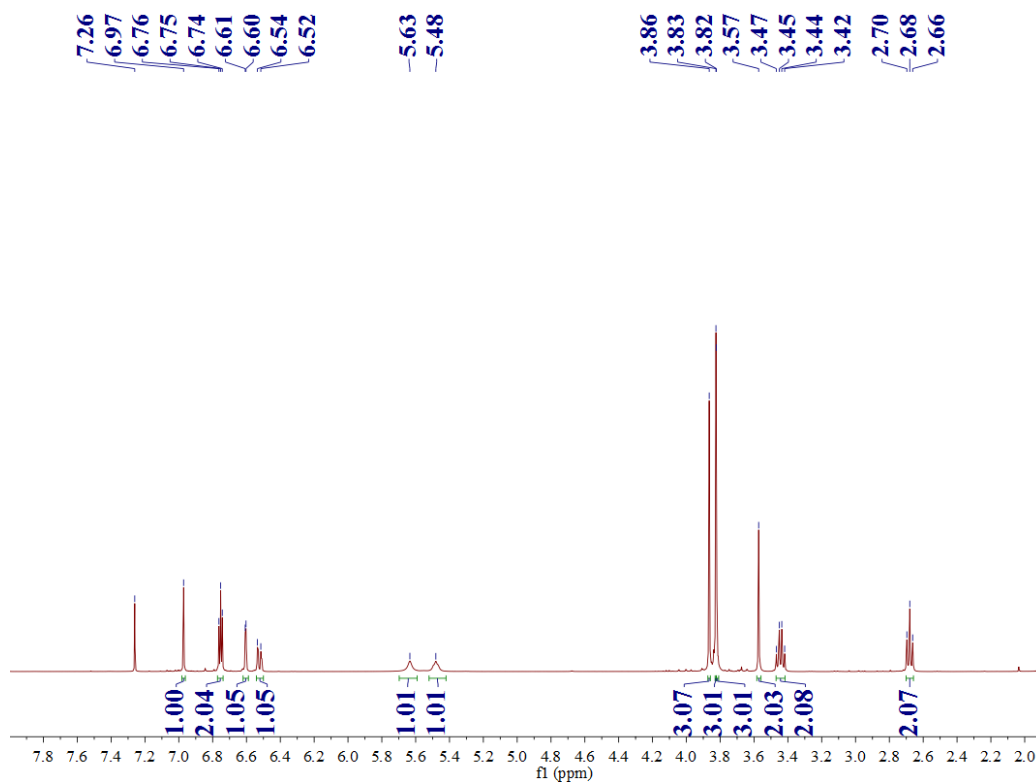


Figure S10. ¹H NMR (400MHz, Chloroform-d) for (1)

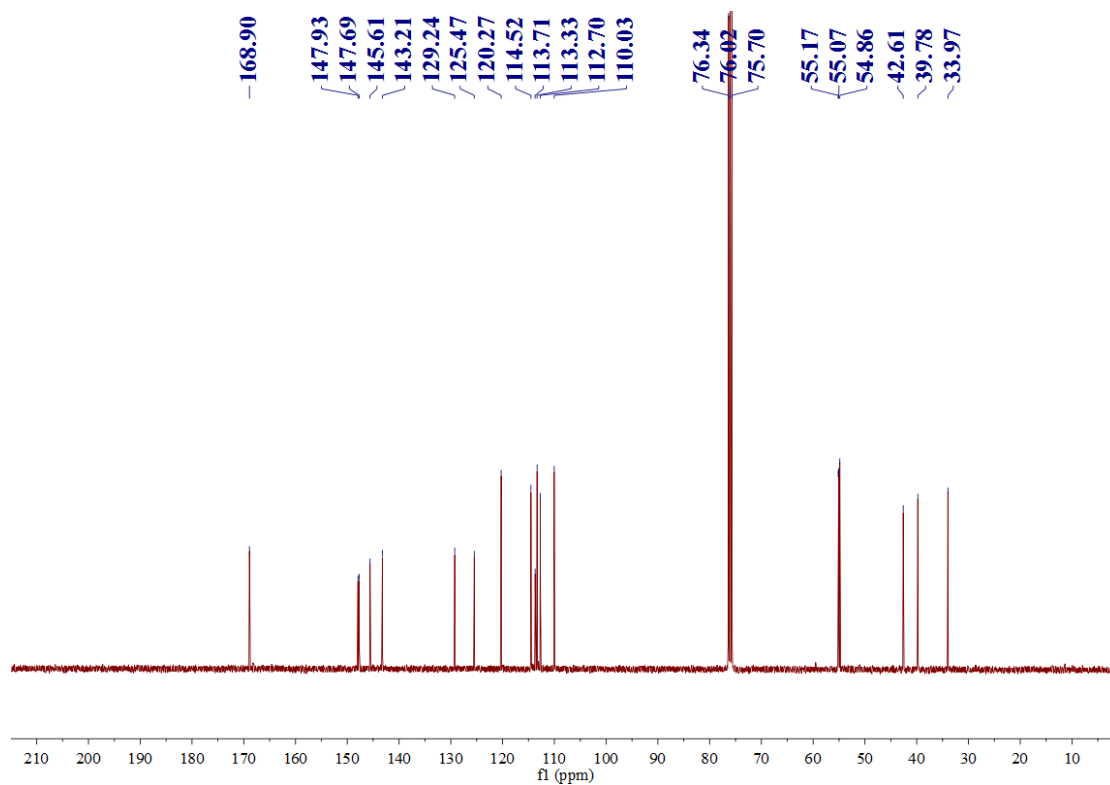


Figure S11. ¹³C NMR (100MHz, Chloroform-d) for (1)

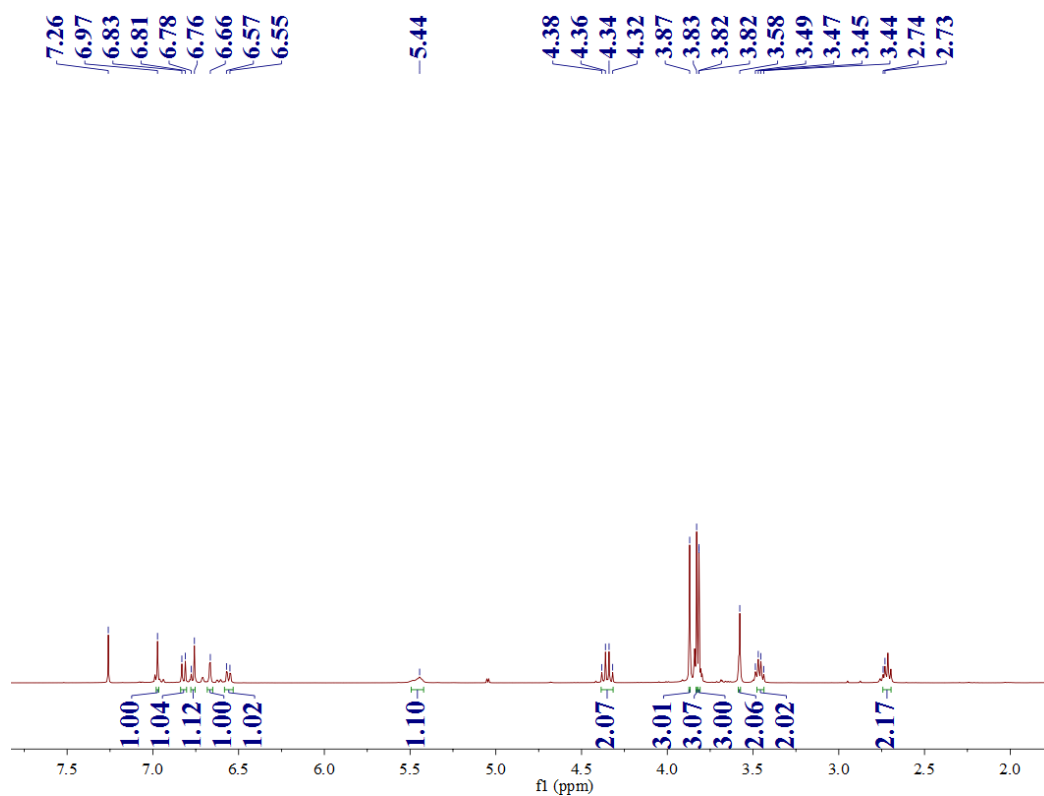


Figure S12. ^1H NMR (400MHz, Chloroform-d) for (2)

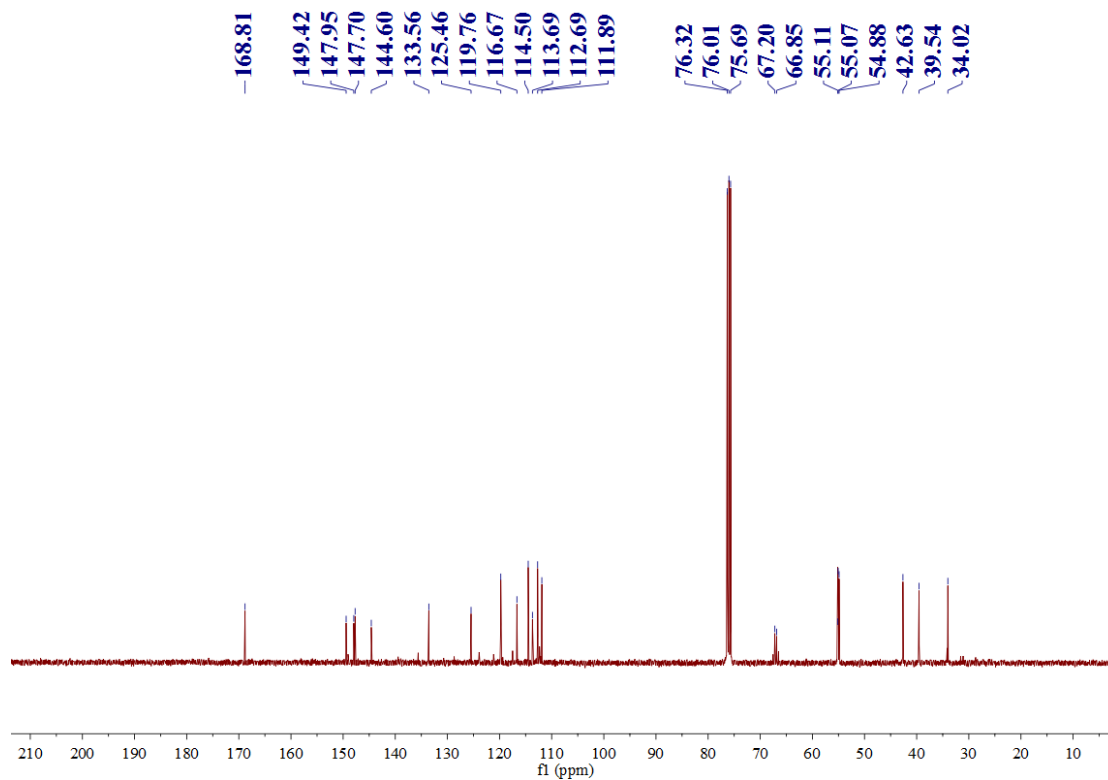


Figure S13. ^{13}C NMR (100MHz, Chloroform-d) for (2)

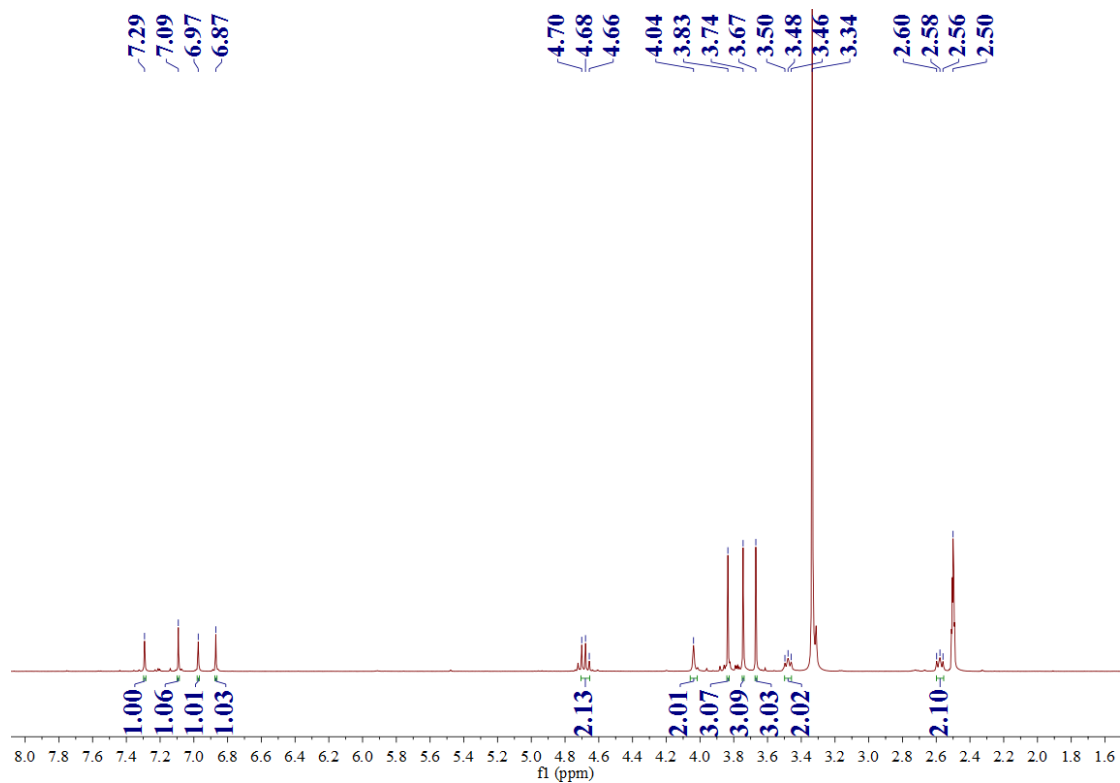


Figure S14. ¹H NMR (400MHz, DMSO-d₆) for (3)

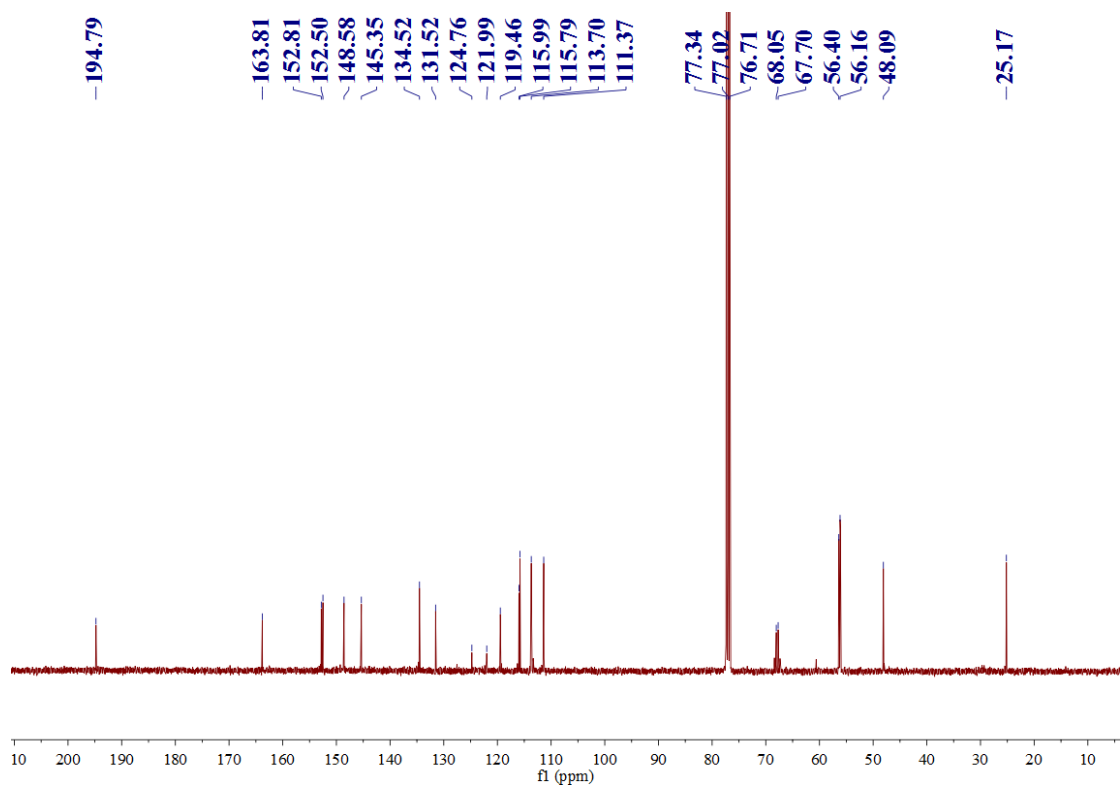


Figure S15. ¹³C NMR (100MHz, Chloroform-d) for (3)

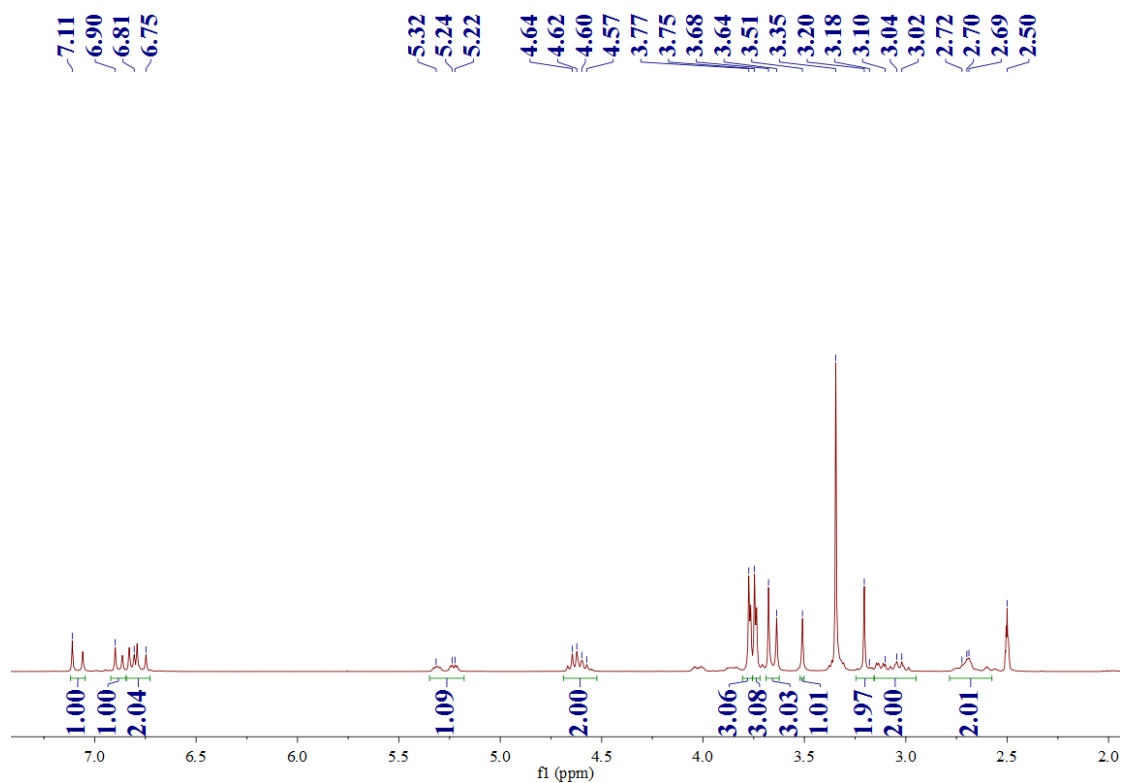


Figure S16. ^1H NMR (400MHz, DMSO-d_6) for (4)

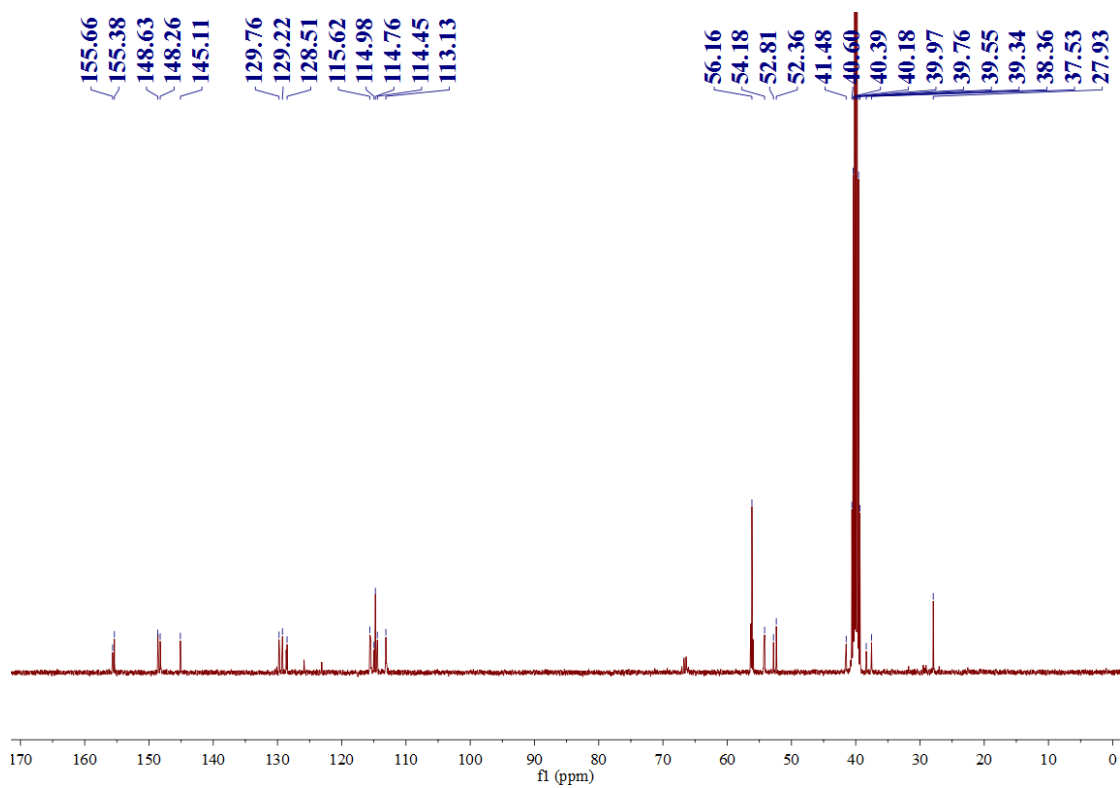


Figure S17. ^{13}C NMR (100MHz, DMSO-d_6) for (4)

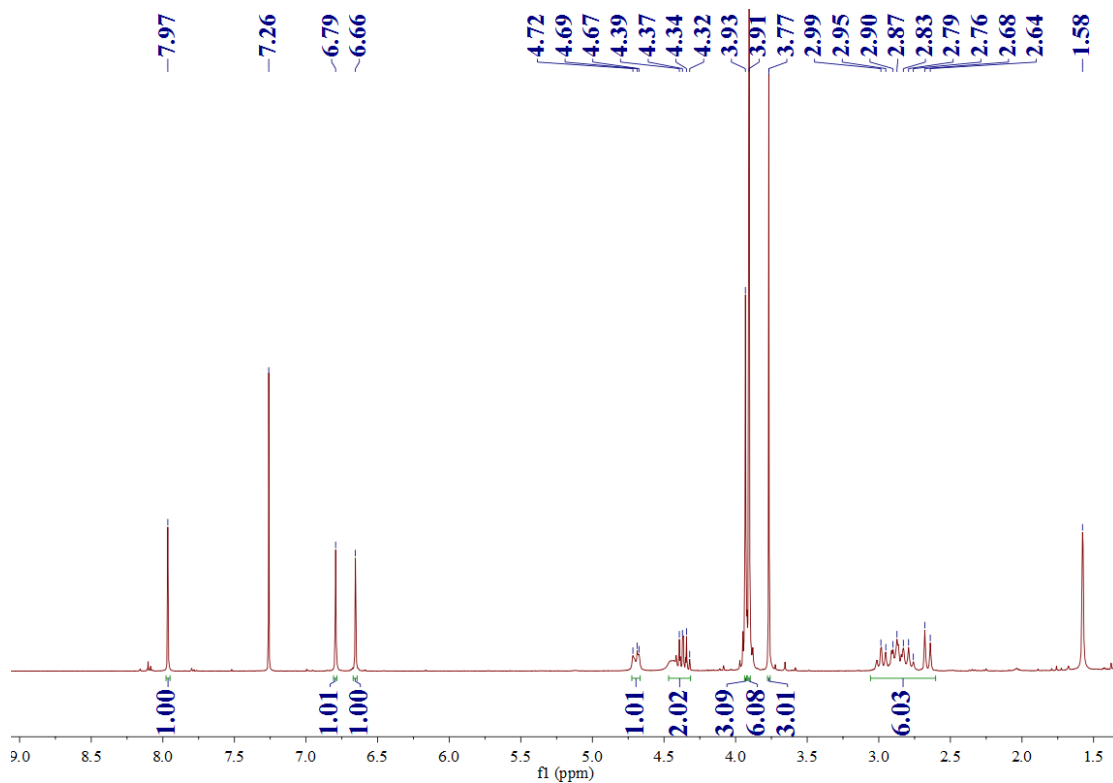


Figure S18. ^1H NMR (400MHz, Chloroform-d) for (6)

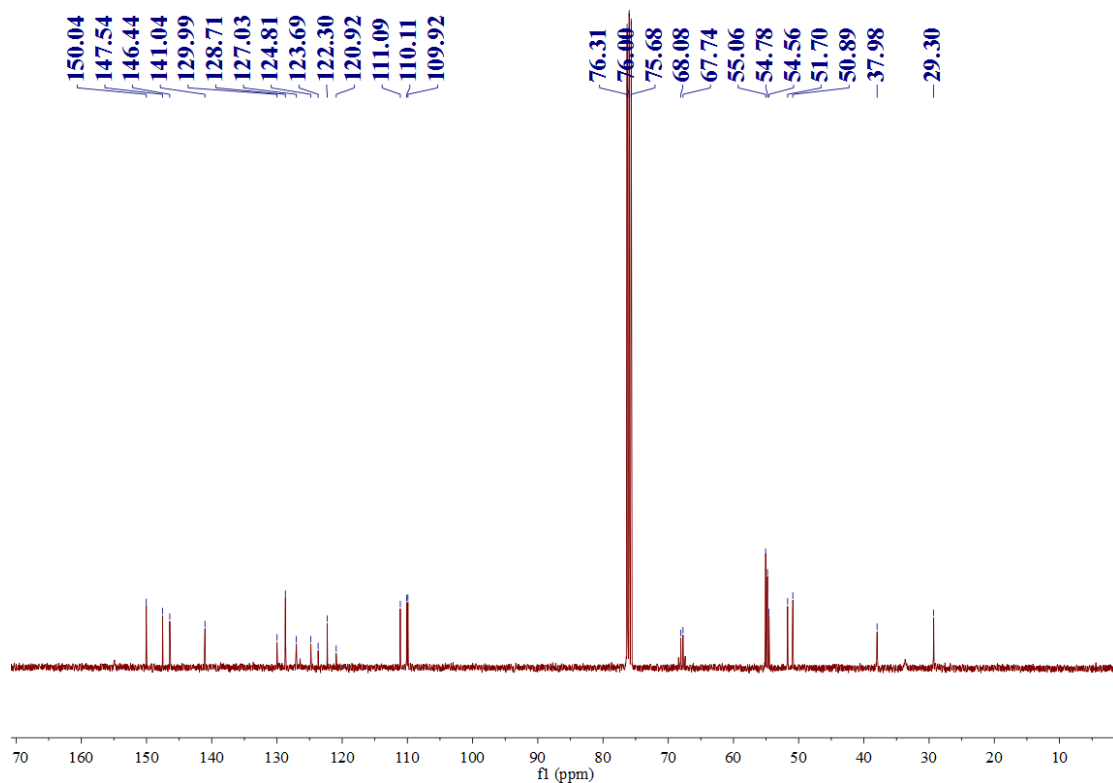


Figure S19. ^{13}C NMR (100MHz, Chloroform-d) for (6)

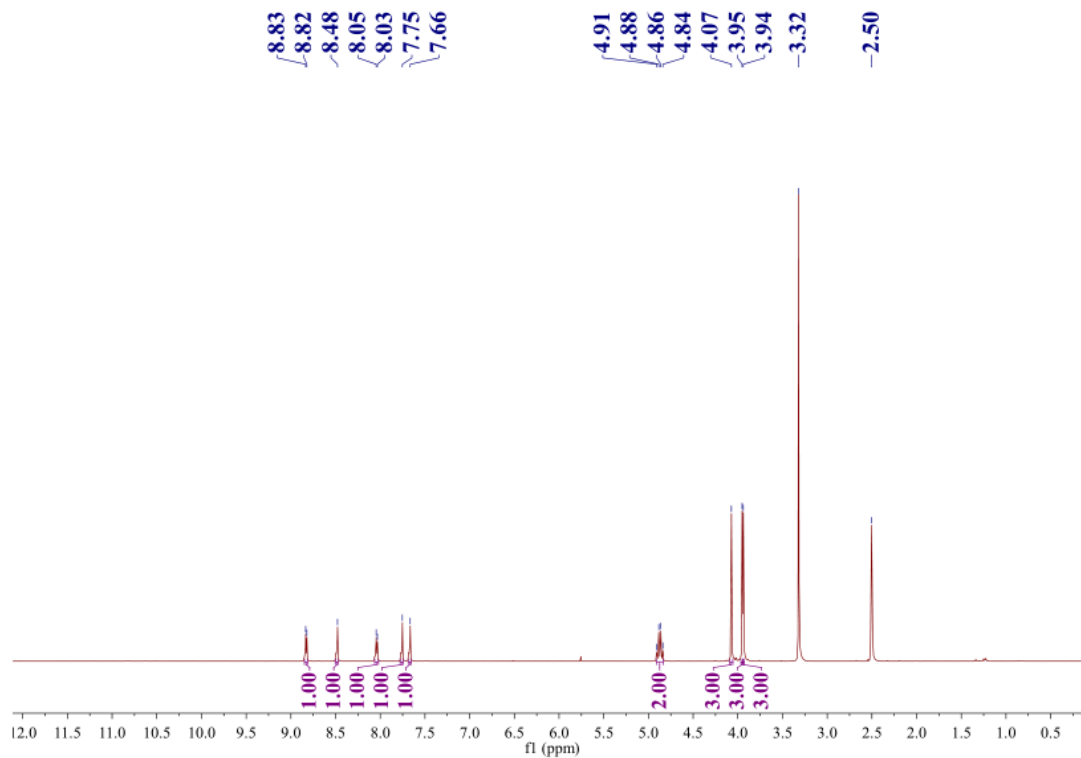


Figure S20. ^1H NMR (400MHz, DMSO- d_6) for L

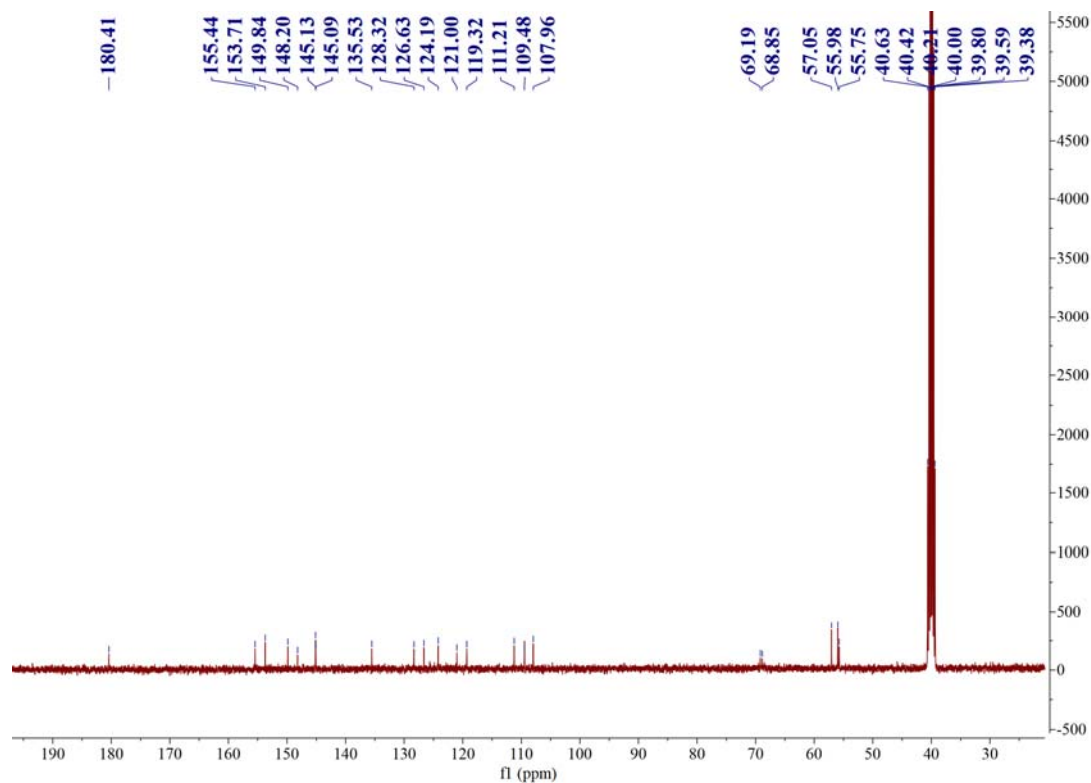


Figure S21. ^{13}C NMR (100MHz, DMSO- d_6) for L

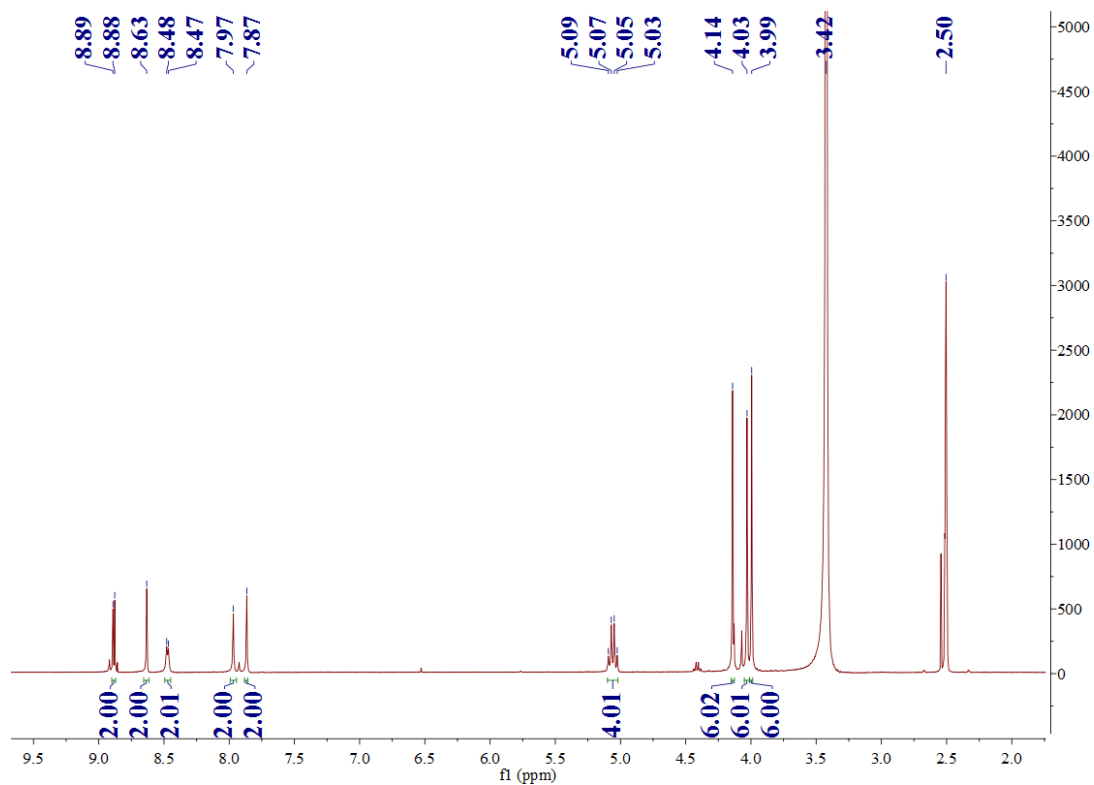


Figure S22. ^1H NMR (400MHz, DMSO-d_6) for complex 3

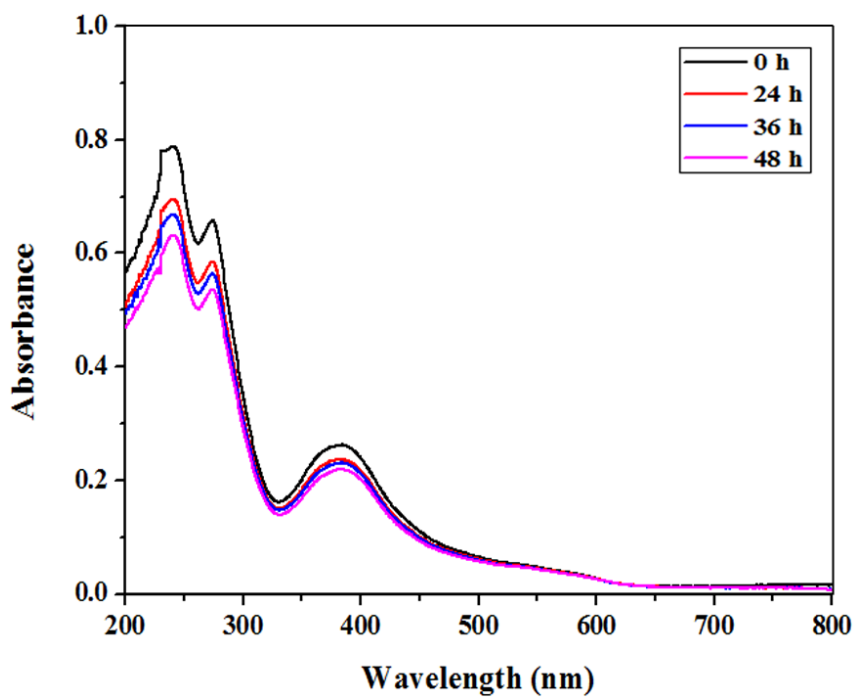


Figure S23. UV-Vis absorption spectra of complex 1

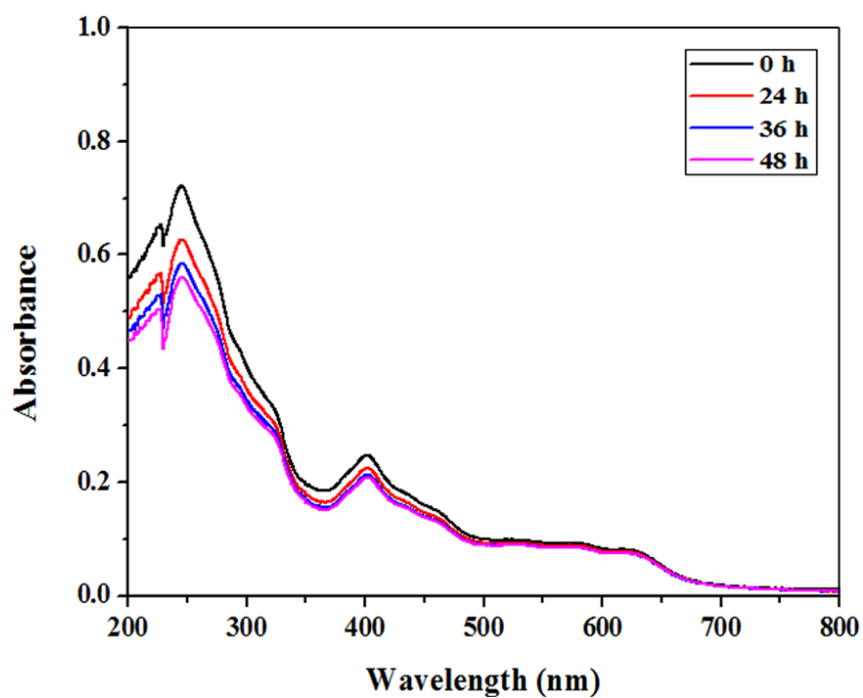


Figure S24. UV-Vis absorption spectra of complex 2

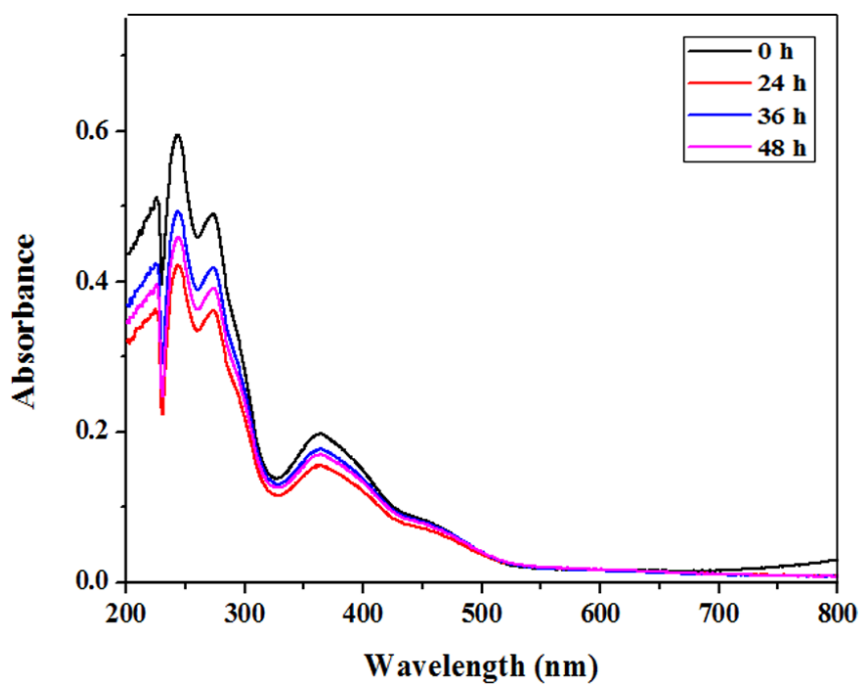


Figure S25. UV-Vis absorption spectra of complex 3

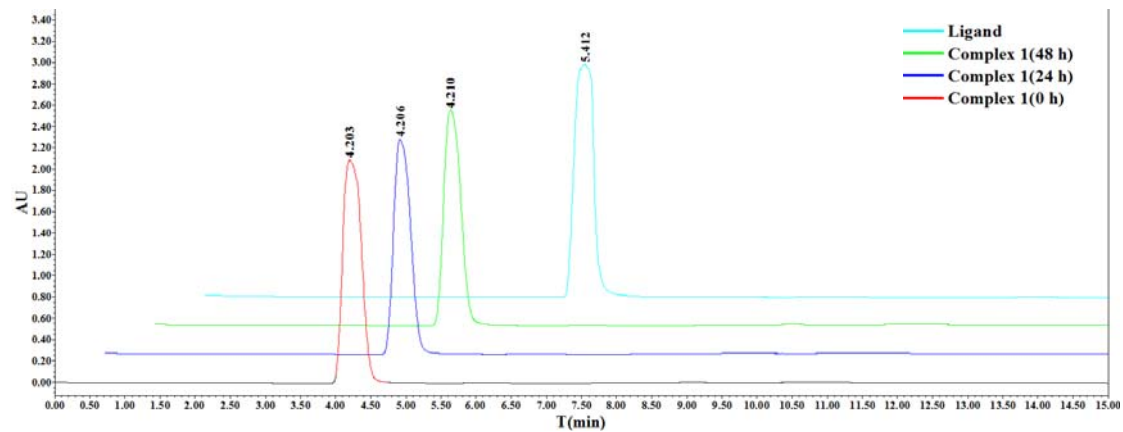


Figure S26. HPLC spectra for complex 1 in DMSO stock solution

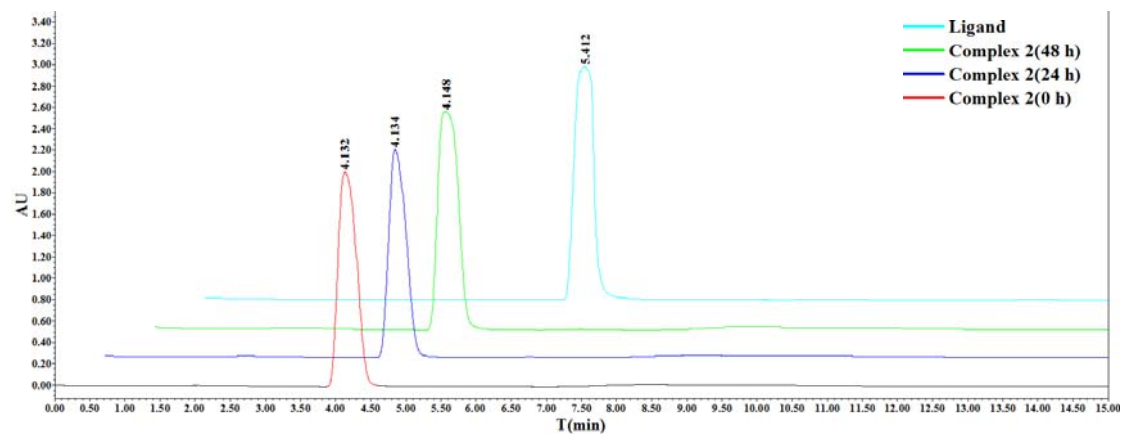


Figure S27. HPLC spectra for complex 2 in DMSO stock solution

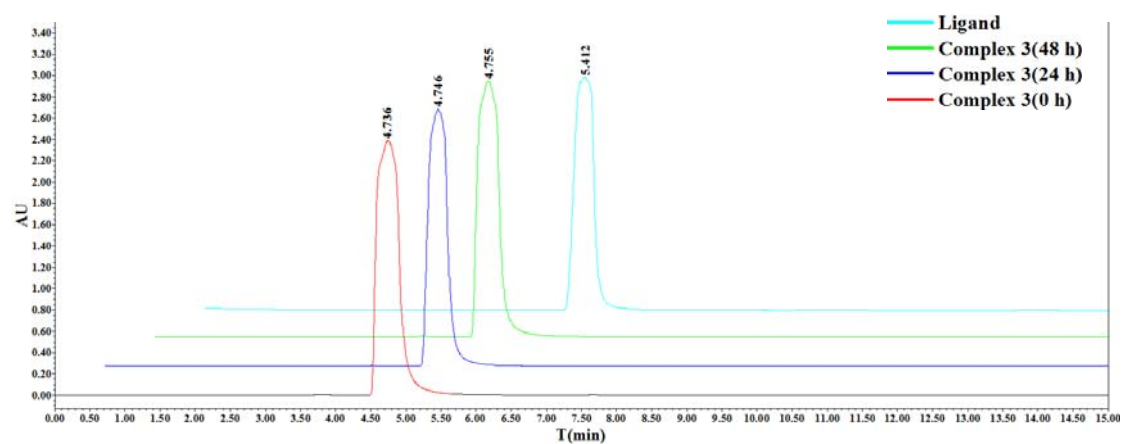


Figure S28. HPLC spectra for complex 3 in DMSO stock solution

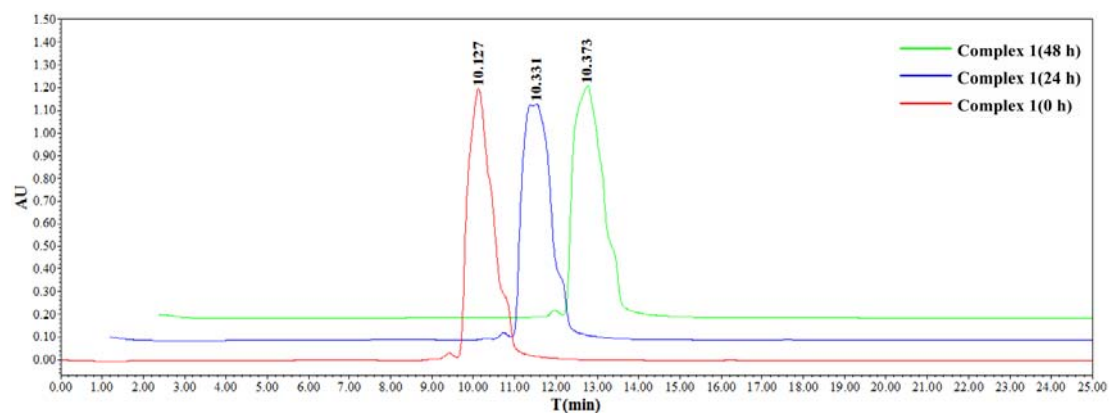


Figure S29. HPLC spectra for complex 1 in TBS solution

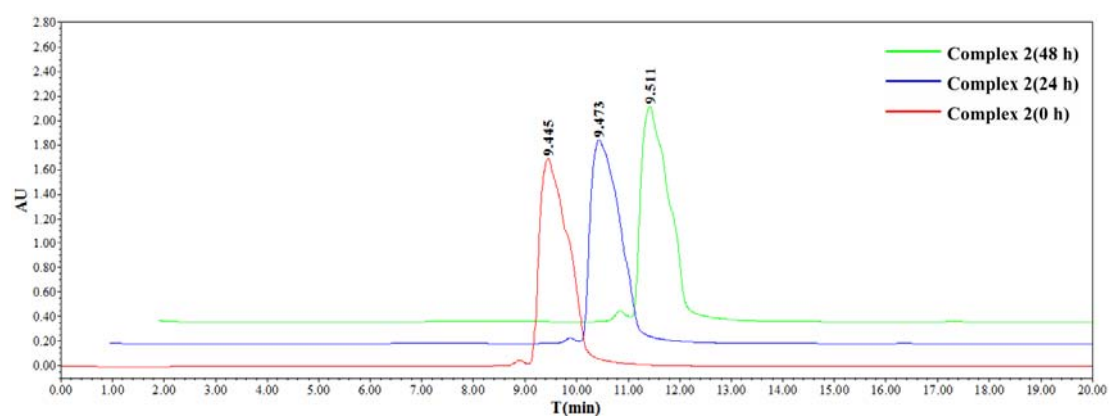


Figure S30. HPLC spectra for complex 2 in TBS solution

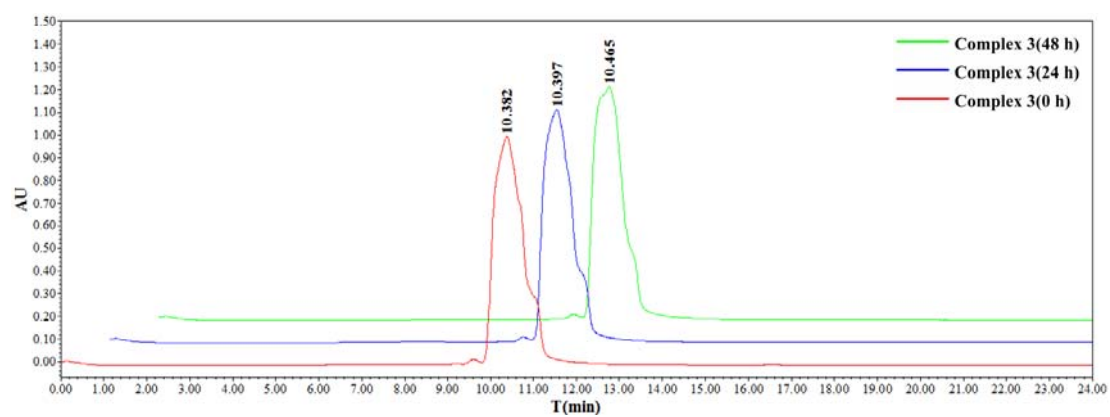


Figure S31. HPLC spectra for complex 3 in TBS solution

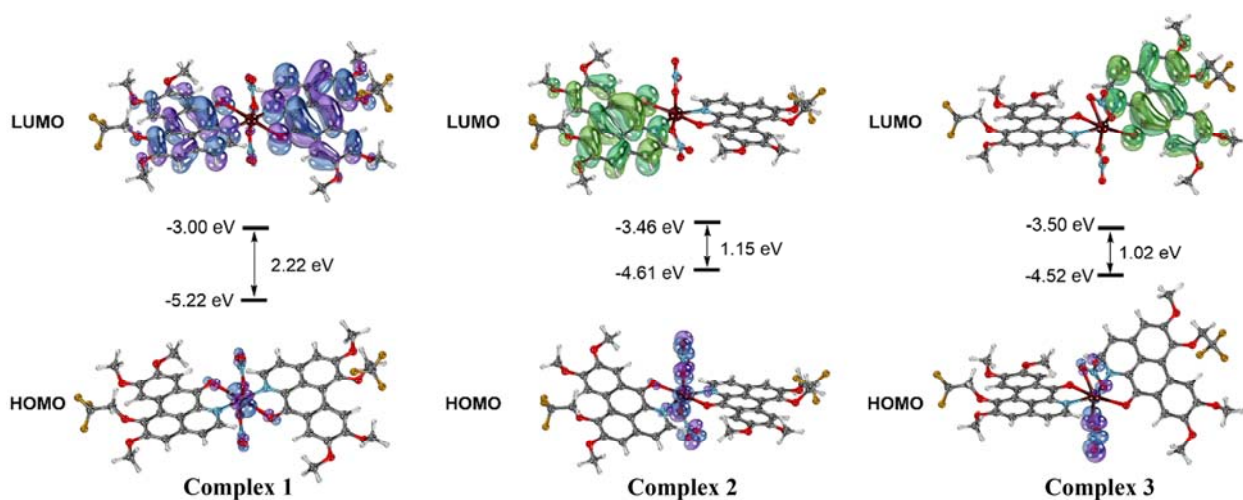


Figure S32. The DFT calculated HOMO-LUMO gap of complexes **1–3** at M06-L/def2svp level of theory.

Table S9. The metal amount (Ni, Cu or Zn) of T-24 cancer cells in different organelles was determined by ICP-MS.

	Cytoskeletal Fraction (ng/10 ⁶ cells)	Mitochondrial Fraction (ng/10 ⁶ cells)	Nuclear Fraction (ng/10 ⁶ cells)	Membrane Fraction (ng/10 ⁶ cells)
Control (Ni)	0.67	0.67	1.15	0.83
Complex 1 (Ni)	1.02	1.39	1.18	0.85
Control (Cu)	6.40	3.44	5.38	4.41
Complex 2 (Cu)	7.32	5.90	5.64	4.87
Control (Zn)	16.58	14.21	9.96	18.11
Complex 3 (Zn)	18.06	26.83	12.61	18.57

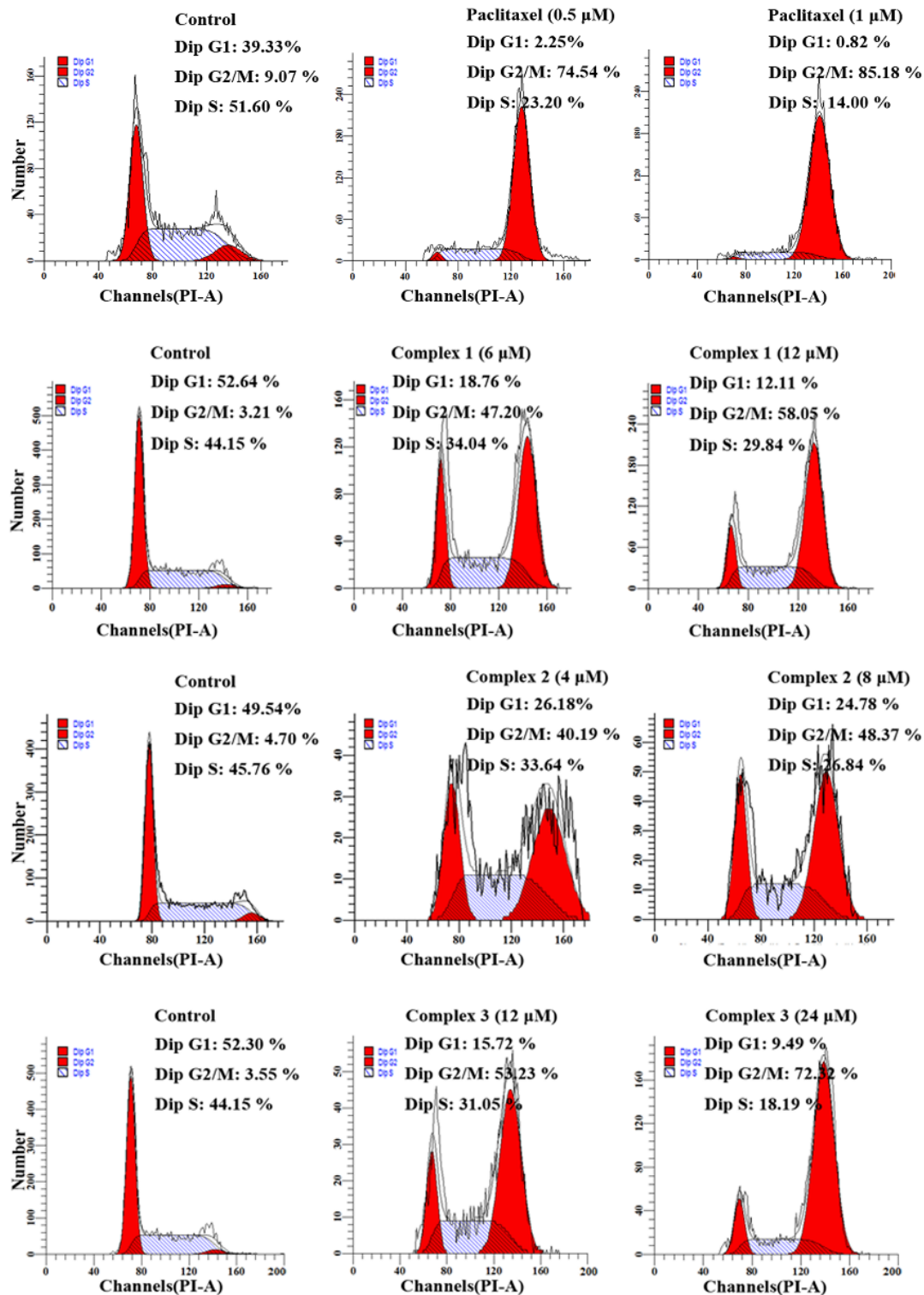


Figure S33. Cell cycle analysis by flow cytometry for the T-24 cells treated with complex 1 (6 and 12 μM), complex 2 (4 and 8 μM) and complex 3 (12 and 24 μM).

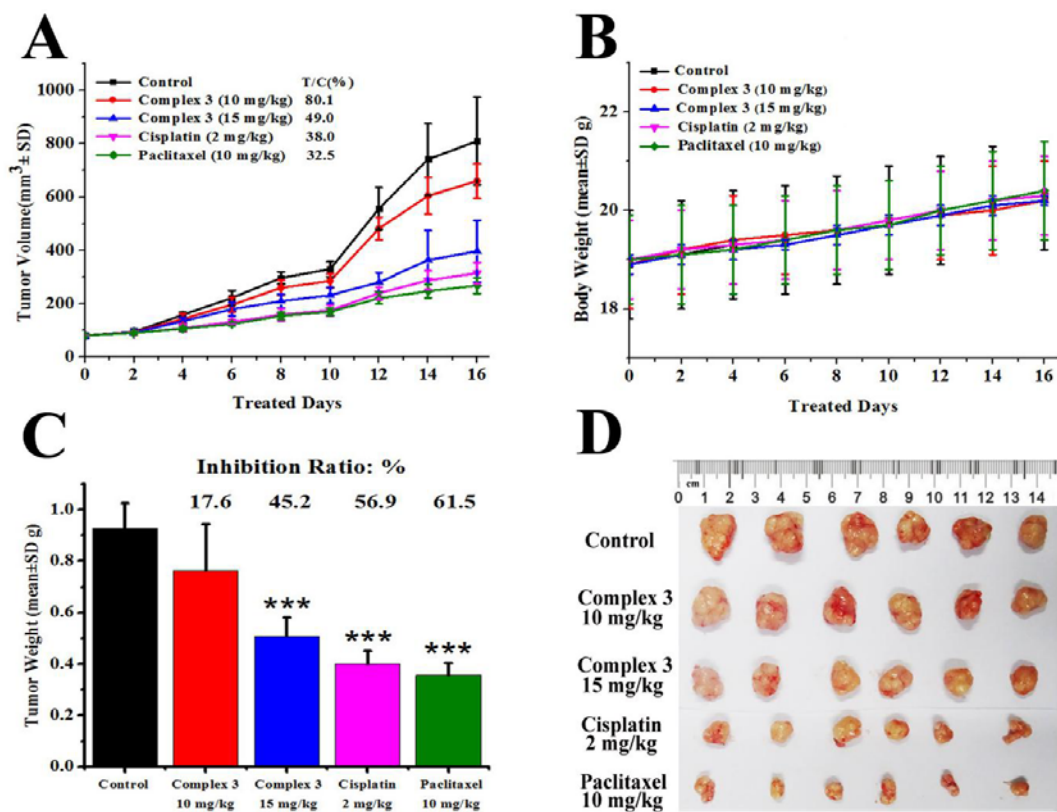


Figure S34. *In vivo* anticancer activity of complex 3 in mice bearing T-24 xenograft. (A) Tumor growth profiles in mice. (B) Body weight change from day 0–16. (C) Tumor weights and inhibition of tumor growth, (***) $P < 0.001$. (D) Photographs of tumor from treatment groups and vehicle group.